JOURNAL OF GEOPHYSICAL RESEARCH, VOL. 99, NO. D6, PAGES 12,897–12,914, JUNE 20, 1994

A model for studying the composition and chemical effects of stratospheric aerosols

Azadeh Tabazadeh, Richard P. Turco and Mark Z. Jacobson
Department of Atmospheric Sciences, University of California, Los Angeles

Abstract. We developed polynomial expressions for the temperature dependence of the mean binary and water activity coefficients for H_2SO_4 and HNO_3 solutions. These activities were used in an equilibrium model to predict the composition of stratospheric aerosols under a wide range of environmental conditions. For typical concentrations of H_2O, H_2SO_4, HNO_3, HCl, HBr, HF, and HOCl in the lower stratosphere, the aerosol composition is estimated as a function of the local temperature and the ambient relative humidity. For temperatures below 200 K, our results indicate that (1) HNO_3 contributes a significant mass fraction to stratospheric aerosols, and (2) HCl solubility is considerably affected by HNO_3 dissolution into sulfate aerosols. We also show that, in volcanically disturbed periods, changes in stratospheric aerosol composition can significantly alter the microphysics that leads to the formation of polar stratospheric clouds. The effects caused by HNO_3 dissolution on the physical and chemical properties of stratospheric aerosols are discussed.

Introduction

Heterogeneous processes on the surfaces of polar stratospheric clouds (PSCs) play a key role in the formation of the ozone hole in the Antarctic [*Solomon et al.*, 1986; *Turco et al.*, 1989]. Moreover, during the past few years, laboratory and modeling studies have shown that heterogeneous reactions on naturally occurring sulfuric acid aerosols may impact ozone on a global scale [*Tolbert et al.*, 1988; *Hofmann and Solomon*, 1989; *Hanson and Ravishankara*, 1991; *Turco and Hamill*, 1992; *Granier and Brasseur*, 1992; *Prather*, 1992]. Following major volcanic eruptions, stratospheric sulfur injection by volcanos can enhance the abundance of sulfate aerosols, creating a source of large-scale ozone depletion. Dissolution and reactions of HCl and other species in volcanic aerosols are crucial to the ozone problem. To address such issues, we have developed a new equilibrium model to calculate solubilities of various species in stratospheric aerosols as a function of local temperature, relative humidity, and the trace composition of the surrounding air.

Considerable amount of laboratory work has been done to measure the solubility of HCl and HNO_3 in sulfuric acid solutions. Solubilities are often expressed in terms of an effective Henry's constant (H^*). H^* is defined as the ratio of the dissolved species in solution to the equilibrium partial pressure of the species over the solution. The laboratory measurements of H^* are either kinetic [*Reihs et al.*, 1990; *Watson et al.*, 1990; *Van Doren et al.*, 1991; *Williams and Golden*, 1993; *Hanson and Ravishankara*, 1993] or equilibrium in nature [*Zhang et al.*, 1993a]. In the kinetic experiments, H^* is calculated indirectly from the measurements of time-dependent uptake coefficient, which varies as a function of the gas accommodation coefficient and liquid-phase diffusion coefficient. Measuring or estimating these coefficients can introduce errors in the extracted value of H^*. However, in the equilibrium method, H^* is calculated directly from equilibrium vapor pressure measurements over a known solution composition. We have used data obtained from the latter technique to validate the solubilities predicted by our model.

Jaecker-Voirol et al. [1990] and *Luo et al.* [1994] have modeled the solubility of HNO_3 and HCl, respectively, in sulfuric acid solutions using HNO_3 and HCl activity coefficients. The activities were extrapolated from laboratory measurements at room temperatures. Here we used recent laboratory measurements [*Zhang et al.*, 1993a, b], along with tables for apparent enthalpy, heat capacity, and activity coefficients to extrapolate room temperature binary activities (solute and solvent) to stratospheric temperatures. We then use these binary activities in a new equilibrium solver (M. Z. Jacobson et al., Simulating equilibrium within aerosols and non-equilibrium between gases and aerosols, submitted to *Journal of Geophysical Research*, 1994) to predict solubilities for various species in H_2SO_4/H_2O and $H_2SO_4/HNO_3/H_2O$ solutions. In sum, we found that, at higher temperatures (> 210 K), stratospheric aerosols are mainly H_2SO_4/H_2O solutions. For T < 200 K, HNO_3 is a major component of these aerosols, and its aqueous concentration increases rapidly as temperature decreases. If aerosols remain supercooled, then ternary solutions of $H_2SO_4/HNO_3/H_2O$ eventually convert to HNO_3/H_2O solutions. We also show that, if volcanic clouds are present when temperatures are < 200 K, then the major HNO_3-containing aerosols are composed of ternary solutions of $H_2SO_4/HNO_3/H_2O$ instead of nitric acid trihydrate (NAT) particles. The impact of HNO_3 dissolution on the solubility and reactivity of HCl in the stratospheric aerosols are discussed.

2. Binary Strong Electrolyte Systems

To describe the equilibrium of strong electrolyte univalent acids in water, we adopted the *Brimblecombe and Clegg* [1988] activity formulation. This model is applied to the

Paper number 94JD00820.
0148-0227/94/94JD-00820$05.00

HNO_3, HCl and HBr binary solutions in water. In the case of H_2SO_4, we used recent laboratory measurements on the properties of H_2SO_4/H_2O solutions to derive new deliquescence curves and activity coefficients for this system [*Zhang et al.*, 1993a, b].

2.1. Univalent Electrolyte Systems

Brimblecombe and Clegg [1988] have shown that, for strong electrolytes in water solutions, the solubility is best described by an equilibrium between the gas phase and the respective ions in solution, given by

$$HA(g) \overset{K_S}{\Leftrightarrow} H^+(aq) + A^-(aq) \tag{1}$$

$$K_S = \frac{m(H^+)m(A^-)\gamma_\pm^2}{P_{HA}} \tag{2}$$

where $m(H^+)$ and $m(A^-)$ are the molal (mole/kilogram of water) concentrations of H^+ and A^- ions in solution, $\gamma_\pm$ is the mean activity coefficient of the electrolyte HA in solution, P_{HA} is the gas pressure and K_S is the overall gas solubility constant (mole^2/kilogram^2-atm). The mean activity coefficient can be determined from thermodynamic models of electrolyte solutions, described below [*Pitzer*, 1991]. From (2), the solubility, S, of HA in a binary solution can be expressed as

$$S = \sqrt{m(H^+)m(A^-)} = \left(\frac{K_S P_{HA}}{\gamma_\pm^2}\right)^{1/2} \tag{3}$$

Thus for a known equilibrium composition (S), the equilibrium vapor pressure over the solution (P_{HA}) is equal to $S^2\gamma_\pm^2 / K_S$. The overall gas solubility constant (K_S) variation with temperature is approximated using the van't Hoff equation

$$\ln\left(\frac{K_{S2}}{K_{S1}}\right) = \frac{\Delta H^o}{R}\left(\frac{1}{T^o} - \frac{1}{T}\right) + \frac{\Delta C_p^o}{R}\left(\frac{T^o}{T} - 1 - \ln\left(\frac{T^o}{T}\right)\right) \tag{4}$$

where ΔH^o (calorie/mole) and ΔC_p^o (calorie/Kelvin-mole) are the enthalpy and the heat capacity changes, respectively, for the process described in (1) at the standard temperature (T^o = 298.15 K). Table 1 lists the appropriate parameters for the electrolyte solutions studied in this work. K_{S2} and K_{S1} are the overall gas solubility constants at temperatures T and T^o, respectively.

The mean activity coefficient, $\gamma_\pm$, in equation (2) can be calculated for a given molality at the standard temperature (T^o) from [*Hammer and Wu*, 1972]

$$\log \gamma_\pm(T^o) = \frac{-0.5108 m^{1/2}}{1 + B^* m^{1/2}} + \beta m + Cm^2 + Dm^3 + Em^4 + Fm^5 \tag{5}$$

where the parameters B^*, β, C, D, E and F are determined experimentally for each electrolyte HA (*Hammer and Wu*, 1972), and m is the molality of HA in solution. These parameters are given in Table 2 for several electrolytes studied here.

Once the mean activity coefficient is determined at the standard temperature, its value at other temperatures can be calculated using temperature extrapolations [*Clegg and Brimblecombe*, 1990]

$$\log \gamma_\pm(T) = \log \gamma_\pm(T^o) + \frac{1}{\nu}(yL_2 - zJ_2 + \Omega\Gamma_2) \tag{6a}$$

$$y = (T^o - T)/(2.303RT^oT) \tag{6b}$$

$$z = T^o y - \log(T^o/T)/R \tag{6c}$$

$$\Omega = T^o(z + 1/2(T - T^o)) \tag{6d}$$

where L_2 (calorie/mole) and J_2 (calorie/mole-Kelvin) are the partial molal enthalpy and heat capacity of the solute, respectively, ν is the number of ions produced by the complete dissociation of one molecule of solute. The term Γ_2 is equal to $\partial J_2 / \partial T$ evaluated at the standard temperature and concentration of interest. The partial molal quantities (L_2 and J_2) are related to the apparent molal quantities ($^\phi L$ and $^\phi C_p$) by [*Clegg and Brimblecombe*, 1990]

$$L_2 = {}^\phi L + m(\partial {}^\phi L / \partial m) \tag{7a}$$

$$J_2 = {}^\phi C_p - {}^\phi C_p^o \tag{7b}$$

where $^\phi C_p^o$ is the apparent molal heat capacity at infinite dilution.

We used the *Handbook of Chemistry and Physics* data [*Lide*, 1990] to express the apparent molal quantities ($^\phi L$ and $^\phi C_p$) as polynomial functions of molality for each electrolyte HA (Tables 3 and 4). We use these polynomial functions along with temperature variations of the overall gas solubility constant (K_S), and equations (2) through (7) to extrapolate room temperature solubilities (3) to low temperatures (< 220 K), typical of the stratosphere.

For a pure binary 1-1 electrolyte system at standard temperature, the water (a_w) activity is related to the osmotic coefficient, ϕ, by [*Pitzer*, 1991]

$$\ln a_w(T^o) = -0.036\phi(T^o)m \tag{8a}$$

$$\phi(T^o) = 1 + \frac{1}{m}\int_0^m m\left(\frac{d \ln \gamma_\pm(T^o)}{dm}\right)dm \tag{8b}$$

where m is the electrolyte molality. The integrand in (8b) can be calculated if the mean activity parameters are known from

Table 1. Thermodynamic Parameters

Species	K_S, mol^2/kg^2 atm	ΔC_p^o, cal / K mo	ΔH^o, kcal mol
HNO_3	2.45e+6	-3.34704e+1	-1.74713e+1
HCl	2.04e+6	-3.95793e+1	-1.78967e+1
HBr	1.32e+9	-9.76820e+0	-2.03537e+1

Parameters were taken from *Brimblecombe and Clegg* [1988]. Read 2.45e+6 as 2.45x10^6.

Table 2. Activity Parameters

Species	Molality Range	B^*	β	C	D	E	F
HNO_3	0-28	1.5824	6.2432e-2	-1.3137e-3	-1.2886e-5	4.917e-7	0.0
HCl	0-16	1.5250	1.0494e-1	6.5360e-3	-4.2058e-4	-4.070e-6	5.258e-7
HBr	0-10	1.6468	1.2457e-1	8.8530e-3	2.4750e-5	-3.719e-5	0.0

Parameters were taken from *Hammer and Wu* (1972). Read 6.2432e-2 as 6.2432×10^{-2}.

(5). The integrated form of equation (8b) is given by *Hammer and Wu* [1972]. The water activity at other temperatures is related to the water partial molal enthalpy (L_1), and heat capacity (J_1) by [*Clegg and Brimblecombe*, 1992]

$$\log a_w(T) = \log a_w(T^o) + yL_1 - zJ_1 + \Omega\Gamma \tag{9}$$

where the term Γ_1 is equal to $\partial J_1 / \partial T$ evaluated at the standard temperature and concentration of interest, and the partial water molal quantities are related to the apparent molal quantities ($^\phi L$ and $^\phi C_p$) by [*Clegg and Brimblecombe*, 1990]

$$L_1 = -0.018m^2(\partial {}^\phi L / \partial m) \tag{10a}$$

$$J_1 = -0.018m^2(\partial {}^\phi C_p / \partial m) \tag{10b}$$

For atmospheric applications, the water activity is equal to the ambient relative humidity, which is defined as the ratio of water vapor partial pressure to the water vapor saturation pressure. Thus for a constant water vapor pressure profile, the temperature variation of water activity over a binary solution can be calculated if the saturation vapor pressure of water is known. For temperatures below 250 K, the saturation vapor pressure of water in units of torr is given as [*Clegg and Brimblecombe*, 1990]

$$P^{sat}_{H_2O} = \exp\{23.630958 - 5832.42478/T - (1.01358x10^{-5})T^2\} \tag{11}$$

Solving equations (8) through (11) analytically for the pure electrolyte molality, the deliquescence curves can be computed for various binary solutions in water. The deliquescence curve describes the quantitative relationship between temperature and the equilibrium binary solution composition for a constant water vapor pressure profile.

In most binary equilibrium vapor pressure measurements, the aqueous electrolyte concentration is usually expressed either as weight percent or mole fraction. For application in the model described above, all the concentration units need to be converted to molalities. There are simple relations between molality, weight percent, and mole fraction, given by

$$m = \frac{1000W}{M(100-W)} = \frac{1000X}{18(1-X)} \tag{12}$$

where W and X are the weight percent and mole fraction of the electrolyte in solution, respectively, and M is the electrolyte molecular weight in grams.

2.1.1. HNO_3/H_2O system. For this system, we compared model predictions of the HNO_3 and H_2O vapor pressures over nitric acid solutions to the low-temperature measurements of *Hanson and Mauersberger* [1988a] and *Hanson* [1990]. We used (2) through (7) to calculate the vapor pressure of HNO_3 over HNO_3/H_2O solutions for a known composition (S). For computations, the Γ_2 function for HNO_3/H_2O system is given by [*Clegg and Brimblecombe*, 1990]

$$\Gamma_2 = 0.4236x_I(x_I - 2) - 0.08484x_I^{2.5}(5x_I - 7) \tag{13}$$

where x_I, the mole fraction of all ions (H^+ and NO_3^-) in solution, is related to the HNO_3 molality (m) in solution by

$$x_I = \frac{2m}{2m + 55.556} \tag{14}$$

Figure 1a shows the results of our calculations. The dashed lines are least squares fits for the vapor pressure of nitric acid over HNO_3/H_2O solutions, taken form *Hanson and Mauersberger* [1988a] and *Hanson* [1990]. Our results are in excellent agreement with respect to the HNO_3 vapor pressure over this binary solution. For simple application, we have fit

Table 3. Apparent Enthalpy

	$^\phi L = a_o + a_1 m + a_2 m^2 + a_3 m^3 + a_4 m^4 + a_5 m^5$					
Species	a_o	a_1	a_2	a_3	a_4	a_5
HNO_3	5.7200068e+1	-5.4128777e+0	1.4870927e+1	-6.6184600e-1	1.20959091e-2	-8.0648265e-5
HCl	7.2685004e+1	2.2199006e+2	4.5003161e+0	-3.3699633e-1	8.44789761e-3	-7.1967069e-5
HBr	2.2684938e+2	9.8258222e+1	1.2064140e+1	-3.4513187e-1	3.14050852e-3	-3.7356295e-6

Polynomials were fitted to *Lide's* [1990] data on the apparent enthalpy for solute molalities > 1. Read 5.7200068e-1 as 5.7200068×10^1.

Table 4. Apparent Heat Capacity

	$^{\phi}C_p = b_o + b_1 m + b_2 m^2 + b_3 m^3 + b_4 m^4 + b_5 m^5$					
Species	b_o	b_1	b_2	b_3	b_4	b_5
HNO_3	-2.0103909*e*+1	7.7423887*e*+0	-5.6638380*e*-1	2.0842130*e*-2	-3.7501139*e*-4	2.6149276*e*-6
HCl	-3.1787735*e*+1	6.6553697*e*+0	-1.4355236*e*+0	1.8361194*e*-1	-1.1043527*e*-2	2.4811100*e*-4
HBr	-3.3252952*e*+1	5.6691907*e*+0	-7.9187247*e*-1	7.3203752*e*-2	-3.2890892*e*-3	5.4783763*e*-5

Polynomials were fitted to *Lide's* data [1990] on the apparent heat capacity for solute molalities > 1. Read -2.0103909*e*+1 as -2.0103909 x 10^1.

the model generated mean activity coefficient results into a polynomial function in HNO_3 molality (m_N), given by

$$\ln \gamma_N^o = \sum_{i=0}^{5} a_{ni}(T) m_N^i \qquad (15)$$

where the γ_N^o is the HNO_3 mean activity coefficient, and a_n variables are temperature coefficients given in Table 5. Note that from now on equation (15) is used to calculate the mean activity coefficient for HNO_3 instead of equations (5) through (7).

To calculate the equilibrium H_2O vapor pressure, we solved the water activity equation for a known solution composition and temperature from (8). The equilibrium water vapor pressure over the binary system was obtained by multiplying the computed water activity by the water saturation vapor pressure from (11). For computations, the Γ_1 function for HNO_3/H_2O system was [*Clegg and Brimblecombe*, 1990]

$$\Gamma_1 = 0.2390 x_I^2 (0.8861 - 0.8774 x_I^{1.5}) \qquad (16)$$

Model results are compared to low-temperature measurements of *Hanson and Mauersberger* [1988a] and *Hanson* [1990] in Figure 1b. Our results are in good agreement with respect to the water vapor pressure over this binary solution. The deliquescence curves for the HNO_3/H_2O system were calculated from (8) for stratospheric temperatures and humidities. For simple application, we have fit the model-generated water activities into a polynomial function with respect to water vapor pressure (P_w) in units of torr, given by

$$m_N^o = \sum_{i=0}^{5} (-1)^i N_i(T) P_w^i \qquad (17)$$

where m_N^o is the molality for a pure HNO_3/H_2O system, and N variables are temperature coefficients, given in Table 6.

In addition, we also solved (2), (15) and (17) simultaneously to calculate the condensation point (T_c) of HNO_3/H_2O solutions in the stratosphere, given by

$$T_c = \frac{B(P_{H_2O})}{A(P_{H_2O}) - \ln P_{HNO_3}} \qquad (18)$$

where P_{H_2O} and P_{HNO_3} are ambient H_2O and HNO_3 vapor pressures in units of torr, and A and B are pressure coefficients given in Table 7. Figure 2 shows condensation points of aqueous HNO_3 solutions as a function of H_2O and HNO_3 vapor pressures. Note that under typical stratospheric conditions (P_{H_2O} ~ 2 - 3 x 10^{-4} torr and P_{HNO_3} ~ 2 - 8 x 10^{-7} torr), the condensation point of HNO_3/H_2O solutions are ~ 191 - 193 K (Figure 2). This is about 3 - 4 K lower than the nitric acid trihydrate frost point (~ 195 - 196 K), and is about 1 - 3 K higher than the ice frost point (~ 188 - 190 K) [*Hanson*, 1990].

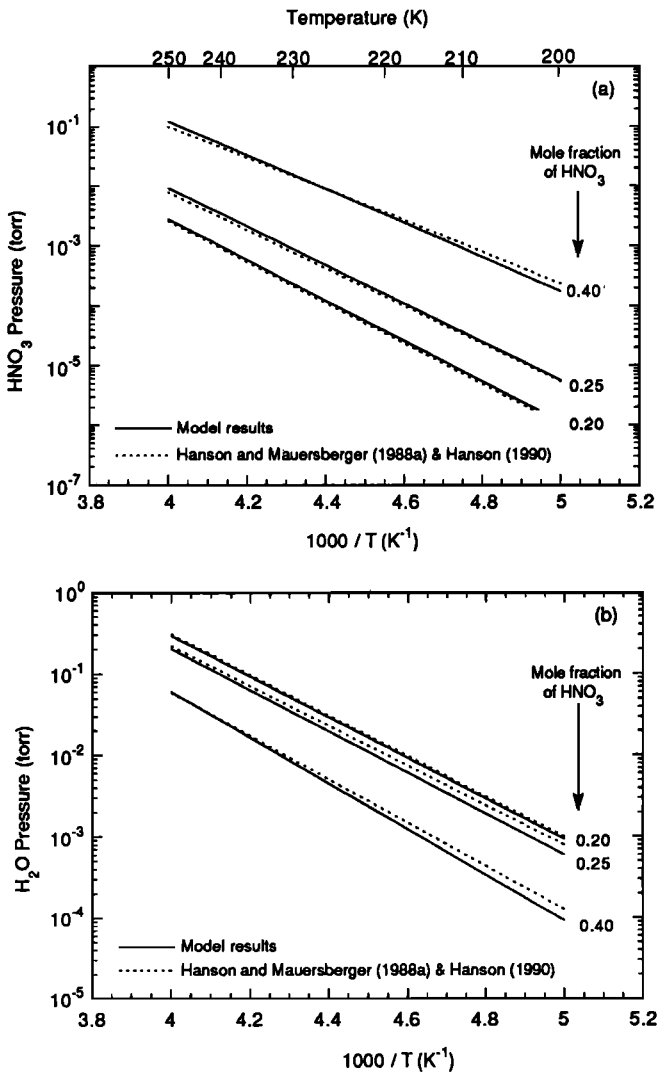

Figure 1. (a) HNO_3 and (b) H_2O vapor pressure over aqueous HNO_3 solutions of various HNO_3 contents. Mole fractions are indicated in the figure. Model results are shown as solid lines, and dashed lines are taken from *Hanson and Mauersberger* [1988a] and *Hanson* [1990].

Table 5. Temperature Dependence for the Activity Parameters

	$a_{ij} = b_o + b_1T + b_2T^2 + b_3T^3 + b_4T^4$				
Coefficients	b_o	b_1	b_2	b_3	b_4
			H_2SO_4 [5 - 15 m]		
a_{so}	-9.8727713620*e*+1	1.5892180900*e*+0	-1.0611069051*e*-2	3.1437317659*e*-5	-3.5694366687*e*-8
a_{s1}	2.6972534510*e*+1	-4.1774114259*e*-1	2.7534704937*e*-3	-8.0885350553*e*-6	9.0919984894*e*-9
a_{s2}	-3.1506575361*e*+0	5.1477027299*e*-2	-3.4697470359*e*-4	1.0511865215*e*-6	-1.2167638793*e*-9
a_{s3}	8.9194643751*e*-2	-1.4398498884*e*-3	9.5874823381*e*-6	-2.8832930837*e*-8	3.3199717594*e*-11
			HNO_3 [0 - 28]		
a_{no}	-9.3085785070*e*-1	1.1200784716*e*-2	-8.7594232370*e*-5	2.9290261722*e*-7	-3.6297845637*e*-10
a_{n1}	-9.9276927926*e*+0	1.3861173987*e*-1	-7.5302447966*e*-4	1.9053537417*e*-6	-1.8847180104*e*-9
a_{n2}	8.9976745608*e*-1	-1.1682398549*e*-2	6.1056862242*e*-5	-1.5087523503*e*-7	1.4643716979*e*-10
a_{n3}	-3.8389447725*e*-2	4.8922229154*e*-4	-2.5494288719*e*-6	6.3306350216*e*-9	-6.1901374001*e*-12
a_{n4}	7.1911444008*e*-4	-8.7957856299*e*-6	4.4035804399*e*-8	-1.0509519536*e*-10	9.8591778862*e*-14
a_{n5}	-5.2736179784*e*-6	6.3762209490*e*-8	-3.1557072358*e*-10	7.4508569217e-13	-6.9083781268*e*-16
			HCl [0 -1 6 m]		
a_{co}	-6.3192805354*e*+1	9.1254642395*e*-1	-5.0869838292*e*-3	1.2864402271*e*-5	-1.2449266080*e*-8
a_{co}	-4.3827430062*e*+0	7.1340939436*e*-2	-4.0096139965*e*-4	1.0068383723*e*-6	-9.7038895012*e*-10
a_{c2}	1.1661208715*e*+0	-1.6494974438*e*-2	9.0259619393*e*-5	-2.2549127848*e*-7	2.1670048131*e*-10
a_{c3}	-2.0032668080*e*-2	2.6583489579*e*-4	-1.4088333815*e*-6	3.4600826715*e*-9	-3.2984375353*e*-12
			HCl [> 16 m]		
a_{co}	1.1359679353*e*+2	-2.1524111207*e*+0	1.60769414070*e*-2	-5.2219047436*e*-5	6.3299312132*e*-8
a_{c1}	-1.6820462678*e*+1	3.1289864756*e*-1	-2.2114878096*e*-3	6.9038174043*e*-6	-8.1334498427*e*-9
a_{c2}	8.0301284717*e*-1	-1.4116783989*e*-2	9.7547869869*e*-5	-3.0341204275*e*-7	3.5788270640*e*-10
a_{c3}	-9.5083850973*e*-3	1.6230303440*e*-4	-1.1001112962*e*-6	3.3912179494*e*-9	-3.9775781303*e*-12

Read -9.8727713620*e*+1 as -9.8727713620 x 10^1.

2.1.2. HCl/H_2O system. For this system, we compare the model predictions of HCl vapor pressure over HCl/H_2O solutions to the measurements of *Fritz and Fuget* [1956]. Using equations (2) through (7), we computed the HCl vapor pressure over solutions ranging from 1 to 37 % HCl by weight. To obtain the results below, we estimated Γ_2 ($\partial J_2 / \partial T$) from the extensive studies of *Holmes et al.* [1987] and *Fritz and Fuget* [1956] on the thermodynamic properties of the HCl/H_2O system, which is

$$\Gamma_2 = -0.7782 - 0.04394m + 0.01126m^2 - 0.0001148m^3 \quad (19)$$

where m is the molality of HCl in solution. The results of our calculations are shown as solid lines in Figure 3, and the dashed lines were taken from *Fritz and Fuget* [1956]. There is good agreement between measurements and calculations. This comparison shows that our low temperature extrapolation from room temperature data worked reasonably well in describing the thermodynamic properties for the HCl/H_2O

Table 6. Temperature Coefficients for HNO_3 Molality

	$\ln N_i(T) = a_o + a_1/T + a_2/T^2 + a_3/T^3 + a_4/T^4$				
Coefficients	a_o	a_1	a_2	a_3	a_4
N_o	2.5757237579*e*-1	3.4615149493*e*+3	-1.1460419802*e*+6	1.6003066569*e*+8	-8.2005020704*e*+9
N_1	-2.3081801501*e*+1	9.7545732474*e*+3	-1.0751476647*e*+6	1.2845681641*e*+8	-5.6387338050*e*+9
N_2	-1.1454916074*e*+2	6.7557746435*e*+4	-1.5833469853*e*+7	2.0068038322*e*+9	-9.5789893230*e*+10
N_3	-3.7614906671*e*+2	2.5721043666*e*+5	-6.9093891724*e*+7	8.8886258262*e*+9	-4.3013954256*e*+11
N_4	-1.1566205559*e*+3	8.5657451707*e*+5	-2.4386088798*e*+8	3.1789555772*e*+10	-1.5566652191*e*+12
N_5	-2.9858872606*e*+3	2.2912842052*e*+6	-6.6825883931*e*+8	8.7835101682*e*+10	-4.3330365673*e*+12

Read 2.5757237579*e*-1 as 2.5757237579 x 10^{-1}.

Table 7. Pressure Coefficients for the Condensation Point of HNO_3/H_2O Solutions

	P_{H_2O} (x 10^4 torr)								
Coefficients	1.0	1.5	2.0	2.5	3.0	3.5	4.0	4.5	5.0
A (x 10^{-2})	1.2891	1.2848	1.3093	1.3287	1.3285	1.3285	1.2956	1.2839	1.3300
B (x 10^{-4})	2.7006	2.7234	2.7883	2.8402	2.8521	2.8626	2.8077	2.7928	2.8901

A and B coefficients are valid for a HNO_3 vapor pressure range of 10^{-8} - 3 x 10^{-6} torr.

system. Note that for comparisons with the experiments, we have used the Clausius-Clapeyron relation to extrapolate *Fritz and Fuget* [1956] data to lower temperatures.

For simple application, we have fit the model-generated mean activity coefficient results for HCl into a polynomial function in HCl molality (m_{Cl}), using equations (5) - (7) and (19). This relation is given as

$$\ln \gamma^o_{Cl} = \sum_{i=0}^{3} a_{ci}(T) m^i_{Cl} \qquad (20)$$

where γ^o_{Cl} is the HCl mean activity coefficient, and a_c variables are temperature coefficients given in Table 5. Note that from here on, equation (20) instead of (5) through (7) is used to calculate the mean activity coefficient for HCl. The activity parameters for the HCl/H_2O system (Table 2) are valid up to only a molality of 16, which is insufficient for most stratospheric applications. Thus we derived new activity parameters for the HCl/H_2O system for molalities > 16 from the ternary vapor pressure measurements over the $H_2SO_4/HCl/H_2O$ system [*Zhang et al.*, 1993a] described below. Further, because HCl has a low solubility in sulfuric acid solutions under stratospheric conditions, its impact on the equilibrium water vapor pressure over these solutions is negligible. Therefore, the deliquescence behavior of the HCl/H_2O system has a negligible impact on the equilibrium composition of stratospheric aerosols compared to the H_2SO_4/H_2O, and HNO_3/H_2O systems.

2.1.3. HBr/H_2O system. Experimental data on the vapor pressure of HBr over aqueous HBr solutions at low temperatures are currently lacking. The room temperature values are predicted accurately by the parameters given in Tables 1 through 4 [*Brimblecombe and Clegg*, 1988; *Lide*, 1990]. We carried out similar calculations to those of HCl and HNO_3 to investigate the solubility behavior of HBr at lower temperatures. For computations, we assumed the same dependence for Γ_2 as we did for HCl (equation (19)). Unfortunately, the activity parameters for the HBr/H_2O system are invalid under stratospheric conditions.

We made a few comparisons between the HCl and HBr system over the range where the HBr parameters are valid. First, comparing the overall solubility constant of HBr and HCl at room temperature (K_S of HBr ~ 1000 x K_S of HCl) to that at 200 K (K_S of HBr ~ 10000 x K_S of HCl) shows that HBr's solubility increases more rapidly with a temperature decrease than HCl's does. Second, the mean activity coefficient of HBr and HCl in solution appear to differ by at most a factor of 10, for an electrolyte molality of about 10. Therefore the mean activity of HBr can be estimated roughly from the mean activity of HCl for cases where the activity parameters of HBr are not valid. Here we made a few assumptions to calculate the HBr mean activity (using the HCl mean activity coefficient times a constant), in order to estimate the solubility of HBr in H_2SO_4 solutions, described below.

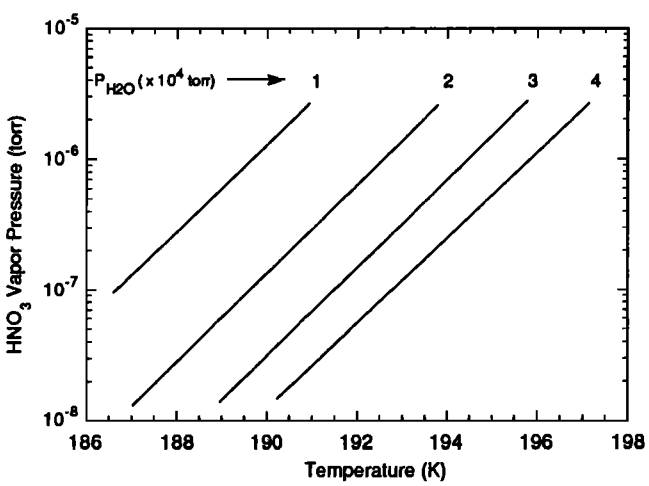

Figure 2. The condensation point of aqueous HNO_3 solutions as a function of H_2O and HNO_3 vapor pressures calculated from (18).

2.2. H_2SO_4/H_2O System

H_2SO_4 in water is a multicomponent electrolyte system in itself. Thus the binary strong electrolyte model discussed

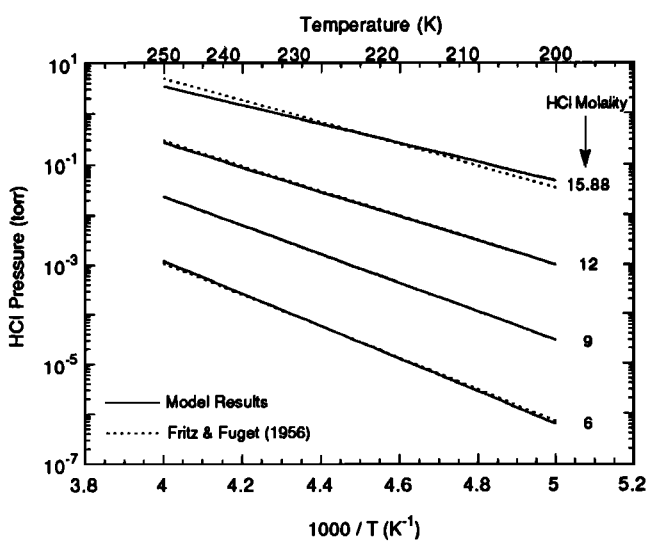

Figure 3. HCl vapor pressure over aqueous HCl solutions of various HCl contents. HCl solution molalities are indicated in the figure. Model results are shown as solid lines, and dashed lines are taken from *Fritz and Fuget* [1956].

above is not applicable to this system. However, *Pitzer et al.* (1977) have successfully treated the thermodynamics of aqueous H_2SO_4 as a mixture of H^+, HSO_4^-, and SO_4^{2-} for concentrations up to 6 molal, and at temperatures close to 25°C. The Pitzer model for H_2SO_4 acid fails under stratospheric conditions for two reasons. First, the molality range for the Pitzer model corresponds to a 0-37% H_2SO_4 solution by weight, and stratospheric aerosols are usually more concentrated. Second, the Pitzer coefficients are valid for a temperature range of 0 to 50°C [*Reardon and Beckie*, 1987], which is out of the stratospheric range.

The thermodynamic properties of the H_2SO_4/H_2O system has been studied by *Gmitro and Vermeulen* [1964], *Steele and Hamill* [1981], *Jaecker-Voirol et al.* [1990] in the past, and more recently by *Zeleznik* [1991] and *Zhang et al.* [1993b]. A survey on the similarities and the differences between these various sources is given by *Zhang et al.* [1993b]. An important conclusion from the laboratory observations on the physical properties for H_2SO_4/H_2O solutions, is that, for $T <$ 210 K and H_2SO_4 weight percents < 60, the H_2SO_4 in solution is nearly completely dissociated into SO_4^{2-} ion [*Zhang et al.*, 1993b; *Middlebrook et al.*, 1993]. We have used this conclusion to derive solute activity coefficients in the $H_2SO_4/HNO_3/H_2O$ ternary system, described below.

Recently, *Zhang et al.* (1993b) have directly measured the water vapor pressure over an equilibrated H_2SO_4 solution (20-70 wt %) at low temperatures. We used their least squares fit for the variation of water vapor pressure over a known solution composition (only seven different compositions) to derive a deliquescence behavior for H_2SO_4/H_2O solutions. For simple application, we have fit the experimental results of *Zhang et al.* [1993b] into a polynomial function with respect to water vapor pressure (P_w) in units of torr, given by

$$W_S^o = \sum_{i=0}^{5} (-1)^i S_i(T) P_w^i \tag{21}$$

where W_S^o is the weight percent for a pure binary sulfuric acid solution, and the S variables are the temperature coefficients given in Table 8. The accuracy of the S coefficients can be increased with more measurements. Note that (21) is valid only for the range where the measurements were carried out (20 - 70 H_2SO_4 wt % at 190-240 K). For higher temperatures, where solutions become more concentrated, equation (21) has less accuracy. Thus for stratospheric applications, we do not recommend using (21) for T > 210 K. Further, we have calculated the binary mean activity coefficient for the H_2SO_4/H_2O system under stratospheric conditions from the activity coefficient data for the HNO_3/H_2O system [*Hammer and Wu*, 1972] and the thermodynamic data for the ternary system of $H_2SO_4/HNO_3/H_2O$ [*Zhang et al.*, 1993a]. The method of calculation is discussed under the multicomponent electrolyte solution section. The results were fitted into a polynomial function in H_2SO_4 molality (m_S), given as

$$\ln \gamma_S^o = \sum_{i=1}^{3} a_{si}(T) m_S^i \tag{22}$$

where γ_S^o is the H_2SO_4 mean activity coefficient, and a_s variables are temperature coefficients given in Table 5.

3. Multicomponent Strong Electrolyte Systems

In principal, the activity coefficient for each electrolyte in a multicomponent system depends on the concentration of all the other species in solution. Thus for a mixed system the equilibrium relation for each binary component from (2) is

$$K_S = \frac{m(H^+)m(A^-)[\gamma_{HA}^{mix}]^2}{p_{HA}} \tag{23}$$

where γ_{HA}^{mix} is the mixed activity coefficient for electrolyte HA in the multicomponent solution. To express γ_{HA}^{mix} for each electrolyte in solution as a function of molality of all other electrolytes in solution is difficult. Thus several researchers have developed empirical methods to calculate the mixed binary activity coefficients from the pure mean binary activity coefficients of all the solutes present in solution [e.g., *Bromley*, 1973; *Kusik and Meissner*, 1978]. Such methods have been applied in equilibrium models to predict the composition of tropospheric aerosols [e.g., *Stelson and Seinfeld*, 1982; *Bassett and Seinfeld*, 1983; *Pilinis and Seinfeld*, 1987].

For the systems of interest here, sulfate/nitrate aerosols, *Bassett and Seinfeld* [1983] showed that the empirical mixing rule of Kusik and Meissner (1978) adequately correlates to experimental data. This rule for the mixed binary activity coefficient (γ_{12}^{mix}) is expressed as

$$\ln \gamma_{12}^{mix} = \frac{z_2}{I(z_1+z_2)}\left[m_2 Z_{12}^2 \ln \gamma_{12}^o + m_4 Z_{14}^2 \ln \gamma_{14}^o + \cdots\right] + \frac{z_1}{I(z_1+z_2)}\left[m_1 Z_{12}^2 \ln \gamma_{12}^o + m_3 Z_{32}^2 \ln \gamma_{32}^o + \cdots\right] \tag{24}$$

Table 8. Temperature Coefficients for H_2SO_4 Weight Percent

	$\ln S_i(T) = a_o + a_1/T + a_2/T^2 + a_3/T^3 + a_4/T^4$				
Coefficients	a_o	a_1	a_2	a_3	a_4
S_o	4.9306007769e+0	-2.8124576227e+2	3.6171943540e+4	-7.3921080947e+5	-1.1640936469e+8
S_1	-1.6902946223e+1	5.7843291724e+3	-1.2462848248e+5	3.1325022591e+7	-2.2068275308e+9
S_2	-3.9722280419e+1	1.2350607474e+4	-3.4299494505e+5	6.2642389672e+7	-3.9709694493e+9
S_3	-5.5968384906e+1	1.2922351288e+4	1.3504086346e+6	-1.7890533860e+8	8.8498119334e+9
S_4	-8.2938840352e+1	2.2079294414e+4	2.9469683691e+5	-3.1424855089e+7	1.0884875646e+9
S_5	-1.0647596744e+2	2.7525067463e+4	4.2061852240e+5	- 5.1877378665e+7	2.2849838182e+9

Read 4.9306007769e+0 as 4.9306007769×10^0.

where the odd and even subscripts refer to cations and anions, respectively, and $Z_{ij}=(z_i+z_j)/2$. γ_{ij}^o is the pure mean binary activity coefficient for a solution containing only ions i and j at the same ionic strength I, given as

$$I=\frac{1}{2}\sum_i z_i^2 m_i \tag{25}$$

where z_i is the absolute value of the charge on species i, and m_i is its molality. Thus to find the activity coefficients in the multicomponent solution with this method one needs to know the binary activity coefficients of all possible pairs of anions and cations in a solution of the same ionic strength.

In atmospheric applications, the water activity in the aqueous phase is equal to the ambient relative humidity. Using this fact along with the Gibbs-Duhem relation for the condition of equilibrium, *Stokes and Robinson* [1965] showed that

$$\sum_k \frac{m_k}{m_k^o}=1 \tag{26}$$

where m_k is the molality of electrolyte k in the multicomponent solution and m_k^o is the pure binary molality calculated at the given ambient relative humidity. We determined the m_k^o functions for H_2SO_4 and HNO_3 binary solutions for a wide range of stratospheric relative humidities, as described above. Including the water equation (26) in the equilibrium calculations discussed below assures that the computed aerosol compositions are in equilibrium with respect to water vapor.

To calculate the equilibrium composition for a multicomponent aqueous system, we solved the following equations simultaneously: (1) the solubility of each electrolyte from (23), (2) the mixed activity coefficients evaluated at I for each electrolyte from (24), (3) the ionic strength from (25), and (4) the water equation at a given humidity from (26). To solve the equations, we used a numerical method described by M. Z. Jacobson et al. (submitted manuscript). This method conserves mass and charge, requires iteration but always converges. The advantage of this method, compared to one using a Newton-Raphson technique, is that it always converges and does not require a first guess.

3.1. $H_2SO_4/HNO_3/H_2O$ System

For this system, we used the ternary equilibrium vapor pressure measurements for HNO_3 over $H_2SO_4/HNO_3/H_2O$ solutions [*Zhang et al.*, 1993b], and the mixed electrolyte model (equation (24)) to derive the mean pure binary activity coefficient of H_2SO_4. In this ternary system, the mixed activity coefficient for HNO_3 (γ_N^{mix}) in solution is related to the HNO_3 vapor pressure (P_{HNO_3}), H_2SO_4 molality (m_S), and HNO_3 molality (m_N) from (23), by

$$\gamma_N^{mix}(T,m_N,m_S)=\left(\frac{P_{HNO_3}K_S(T)}{m(NO_3^-)m(H^+)}\right)^{1/2} \tag{27}$$

Assuming that H_2SO_4 and HNO_3 are completely dissociated into H^+, SO_4^{2-}, and NO_3^-, the ion molalities in solution are $m(NO_3^-)=m_N$, $m(H^+)=m_N+2m_S$ and $m(SO_4^{2-})=m_S$. The nearly complete dissociation of H_2SO_4 into SO_4^{2-} under low temperatures was discussed above. Using (27), and *Zhang et al.*'s [1993a] measurements of HNO_3 vapor pressure over a known ternary solution composition, γ_N^{mix} can be calculated. Also, from (24), γ_N^{mix} for this ternary system is

$$\ln\gamma_N^{mix}=\frac{1}{2I}\left[2(m_N+m_S)\ln\gamma_N^o(T,I)+2.25m_S\ln\gamma_S^o(T,I)\right] \tag{28}$$

where $I=m_N+3m_S$ from (25). Knowing the γ_N^{mix} from (28), and γ_N^o from (15), γ_S^o can be calculated. We calculated the γ_S^o for all the laboratory cases studied by *Zhang et al.* (1993a), and fitted the mean pure activity coefficient data for H_2SO_4 into a polynomial function in sulfuric acid molality given in equation (22). Further, we recalculated the vapor pressure of HNO_3 over a known ternary solution composition from (27), using (15), (22), (28). The model results are shown as solid lines in Figure 4, and the dashed lines are the least squares fits from Zhang et al.

Under stratospheric conditions, the composition of the pure $H_2SO_4/HNO_3/H_2O$ system can be calculated by solving the equilibrium system, described above, for typical abundances of H_2SO_4, HNO_3, and H_2O. Note that for this system, (26) reduces to

$$\frac{m_S}{m_S^o}+\frac{m_N}{m_N^o}=1 \tag{29}$$

where m_S^o, m_N^o are calculated at a given relative humidity from (17) and (21), m_S and m_N are the unknown equilibrium ternary compositions. We assumed that H_2SO_4 is present only in the aqueous phase (H_2SO_4(gas) ~ 0), and the relative humidity stays constant at a given temperature. Thus removal of water vapor by the aerosol phase is neglected (H_2O(gas) ~ const.), which is true for all stratospheric conditions. Model results are shown in Figure 5 for two constant water vapor pressure profiles at ~ 20 km. It is clear that for temperatures below 200 K, HNO_3 is a major component of stratospheric aerosols. In addition, the solubility behavior of HNO_3 in stratospheric aerosols can be divided into three distinct regions (see Figure 5). In region a, HNO_3 is sparsely soluble. In region b, HNO_3 molality in solution (1-10 m) is comparable to H_2SO_4 molality, and in region c, HNO_3 becomes the major component. However, laboratory studies have shown that these ternary systems may freeze in region b or c, which could lead to the nucleation of NAT clouds [*Molina et al.*, 1993]. In a separate paper we investigate the possibility for the existence of supercooled HNO_3/H_2O solutions (region c in Figure 5) under stratospheric conditions (A. Tabazadeh et al., A study of Type I polar stratospheric cloud formation, submitted to *Geophysical Research Letters*, 1994).

Once the equilibrium compositions are known, the effective Henry's constant can be calculated from

$$H^*(T,m_N,m_S)=\frac{m_N}{P_{HNO_3}}=\frac{K_S(T)}{(m_N+2m_S)\left[\gamma_N^{mix}(T,m_N,m_S)\right]^2} \tag{30}$$

where γ_N^{mix} is given by (28). Using the above relation, H^* was plotted as function of T for typical abundances of H_2SO_4 and HNO_3 at about 20 km. The results are shown in Figure 6 for two constant water vapor pressure profiles. Note that H^* depends on the HNO_3 molality (m_N) in a complicated fashion. For example, doubling the HNO_3 abundance in the gas phase would not simply double the aqueous HNO_3 concentration.

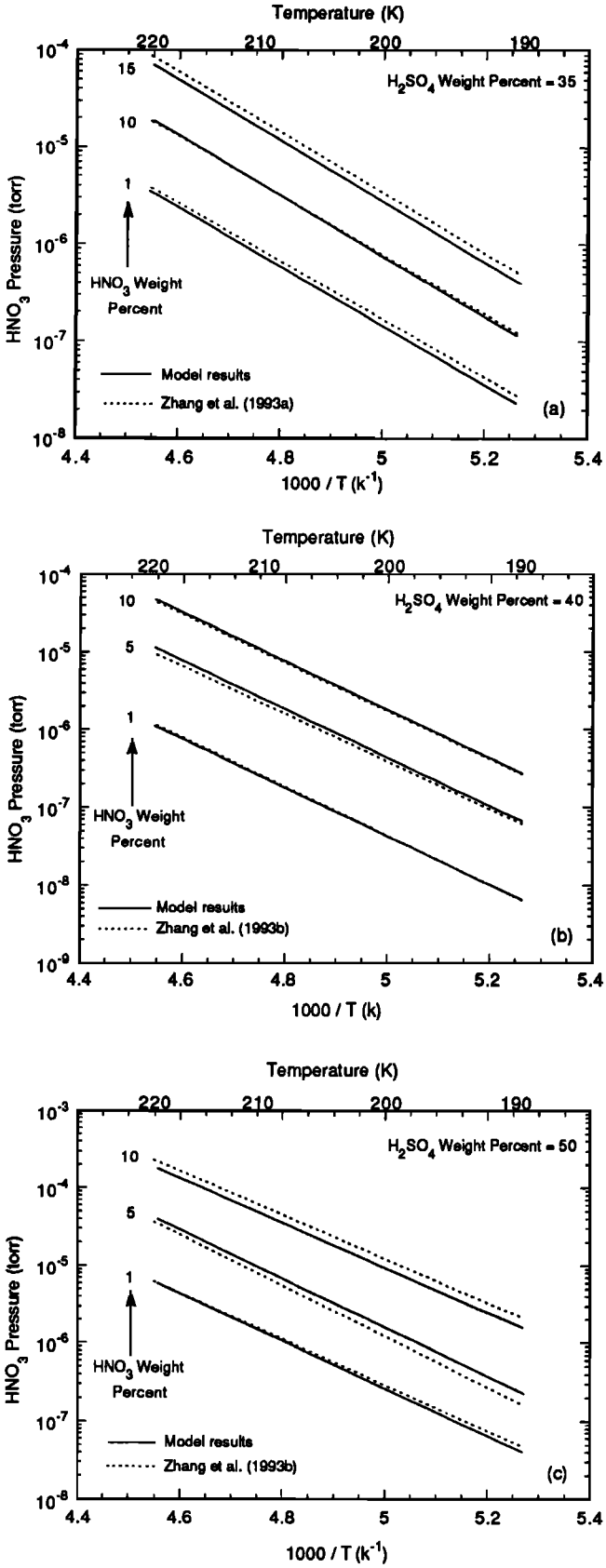

Figure 4. HNO_3 vapor pressure over aqueous H_2SO_4/HNO_3/H_2O solutions of various HNO_3 and H_2SO_4 contents. Weight percents are indicated for each panel in the chart. Model results are shown as solid lines, and dashed lines are taken from *Zhang et al.* [1993a].

Thus it is not possible to express the H^* for HNO_3 in stratospheric aerosols only as a function of sulfuric acid molality and T. However, in region a, where $m_N \sim 0$, there is a linear dependence between the concentration of HNO_3 in the gas and the aqueous phases (Figure 5).

3.2. H_2SO_4/HCl/H_2O System

HCl solubility in sulfuric acid solutions has been recently measured by *Zhang et al.* [1993a]. They determined the equilibrium vapor pressure for HCl over ternary solutions of H_2SO_4/HCl/H_2O. As indicated above, the pure mean binary activity coefficient for HCl (γ^o_{Cl}) is valid up to only 16 molal (Table 2). Thus we used the same procedure as described above to estimate the γ^o_{Cl} for molalities > 16. Using equations (20) and (23), we recalculated the vapor pressure of HCl over this ternary system. Model results are shown as solid lines in Figure 7, and the dashed lines are the least squares fit taken from Zhang et al.

The equations for solving the solubility of HCl in sulfuric acid solutions under stratospheric conditions can be greatly simplified. First, from laboratory observations, the solubility of HCl in sulfuric acid solutions is rather small ($m_{Cl} < 1$). Thus $m_{Cl}/m^o_{Cl} \approx 0$ (where m^o_{Cl} is the pure HCl molality in the binary system, see above), and $m_S = m^o_S$ from (26). Substituting these relations into (23) and (24), the H^* for HCl in pure binary sulfate aerosols is

$$H^*(T, m^o_S) = \frac{m_{Cl}}{P_{HCl}} = \frac{K_S(T)}{2m^o_S\left[\gamma^{mix}_{Cl}(T, m^o_S)\right]^2} \quad (31a)$$

$$\ln \gamma^{mix}_{Cl} = \frac{1}{2I}\left[m^o_S\left(2\ln \gamma^o_{Cl}(I,T) + 2.25 \ln \gamma^o_S(I,T)\right)\right] \quad (31b)$$

where $I = 3m^o_S$, and we assumed that the first term in equation (24) is ~ 0. Using (31), the solubility of HCl in stratospheric sulfate aerosols can be calculated for a wide range of stratospheric humidities. The results are shown in Figure 6 for two constant water vapor pressure profiles.

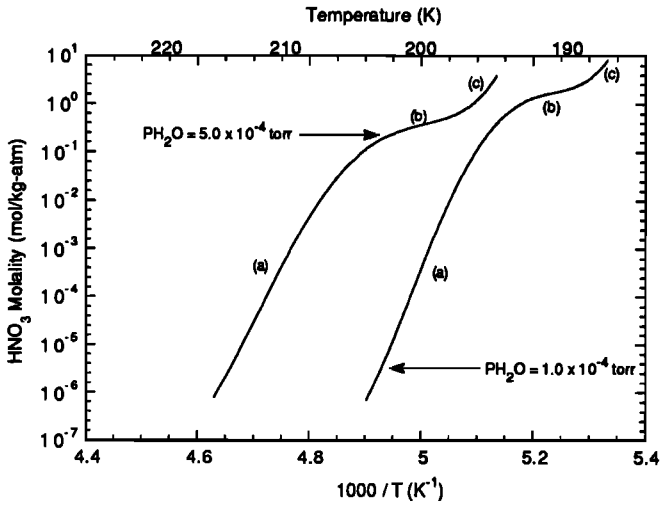

Figure 5. HNO_3 molality in aqueous H_2SO_4 solutions as a function of temperature. Model results are shown for two constant H_2O vapor pressure profiles as indicated in the chart. For model simulations, HNO_3 gas phase concentration was assumed to be 2.0 x 10^{-7} torr. See text for description of various regions labeled in the figure.

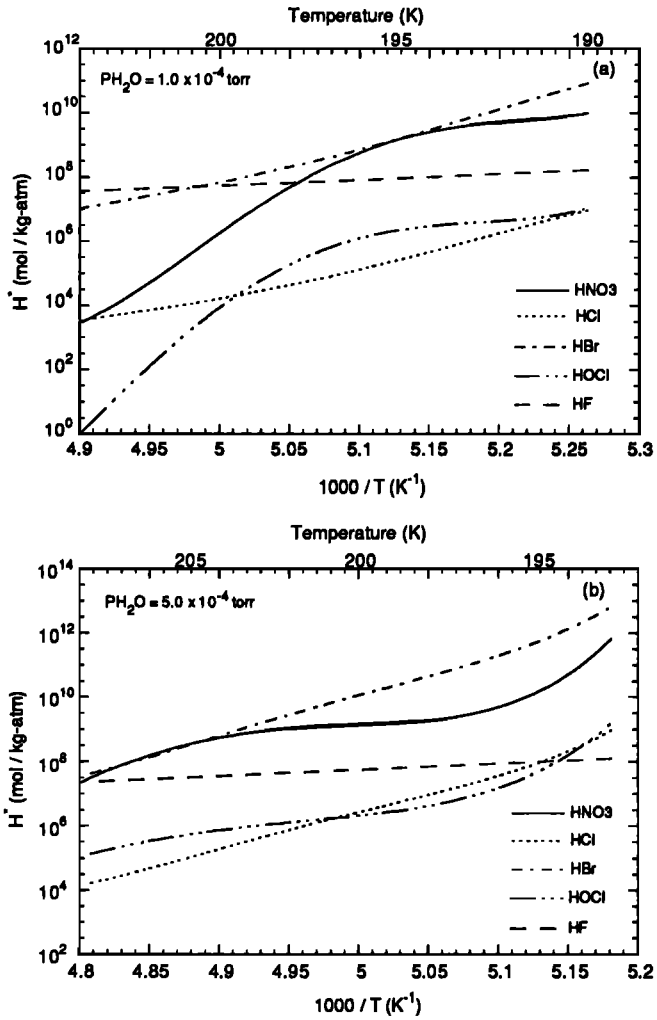

Figure 6. Effective Henry's law constants for various species as a function of temperature in pure aqueous H_2SO_4 solutions. Model results are shown for two constant H_2O vapor pressure profiles as indicated in the chart. For HNO_3 simulations, the HNO_3 gas phase concentration was set at 2.0×10^{-7} torr.

3.3. $HNO_3/HCl/H_2O$ System

Here we compare the ternary system of $H_2SO_4/HCl/H_2O$ to that of $HNO_3/HCl/H_2O$. Although the $HNO_3/HCl/H_2O$ system has not been studied in the laboratory under stratospheric conditions, we have the activity data required to predict HCl solubility in this ternary system. If we assume that stratospheric aerosols are pure HNO_3/H_2O solutions, then the solubility of HCl is approximately

$$H^*(T,m_N^o) = \frac{m_{Cl}}{P_{HCl}} = \frac{K_S(T)}{m_N^o\left[\gamma_{Cl}^{mix}(T,m_N^o)\right]^2} \quad (32a)$$

$$\ln\gamma_{Cl}^{mix} = \frac{1}{2I}\left[m_N^o\left(\ln\gamma_{Cl}^o(I,T) + \ln\gamma_N^o(I,T)\right)\right] \quad (32b)$$

and $I = m_N^o$. Using (31) and (32), we plotted H^* for HCl as a function of temperature in Figure 8. Depending on the humidity and temperature, HCl solubility can be either higher or lower in pure HNO_3/H_2O solutions than in H_2SO_4/H_2O solutions. In the regions of Figure 8 where the solubility of HCl is lower in pure HNO_3/H_2O solutions, actual stratospheric aerosols have insignificant amounts of HNO_3 in the aqueous phase (see Figure 5). Thus HNO_3 in solution will have no impact on HCl solubility. However, in regions where HCl has a higher solubility in pure HNO_3/H_2O solutions, the HNO_3 in solution could perhaps increase the HCl solubility.

3.4. $H_2SO_4/HNO_3/HCl/H_2O$ System

We have solved this system following the procedures outlined above. The effective Henry's constant of HCl is then given by

$$H^*(T,m_N,m_S) = \frac{m_{Cl}}{P_{HCl}} = \frac{K_S(T)}{(m_N+2m_S)\left[\gamma_{Cl}^{mix}(T,m_N,m_S)\right]^2} \quad (33a)$$

$$\ln\gamma_{Cl}^{mix} = \frac{1}{2I}\left[(2m_S+m_N)\ln\gamma_{Cl}^o(I,T) + m_N\ln\gamma_N^o(I,T) + 2.25m_S\ln\gamma_S^o(I,T)\right] \quad (33b)$$

where $I = 3m_S + m_N$. Using the results from the two previous sections and our calculation for this quaternary system, we made a few conclusions about HCl dissolution. The solubility can be well described by (31), where H_2SO_4 is still a major component of the aerosol. Thus so long as H_2SO_4 limits HNO_3 dissolution, HCl solubility is not much different in the $H_2SO_4/HCl/H_2O$ system than it is in the $H_2SO_4/HNO_3/HCl/H_2O$ system. But, when HNO_3 is the major component of the aerosol, HCl solubility could be higher compared to the predictions from (31). In such cases, the solubility of HCl must be directly computed from (33).

3.5. $H_2SO_4/HBr/H_2O$ System

This system has not been studied as extensively in the laboratory as the HCl and HNO_3 ternary systems in H_2SO_4 solutions. The only available measurement suggests that, for

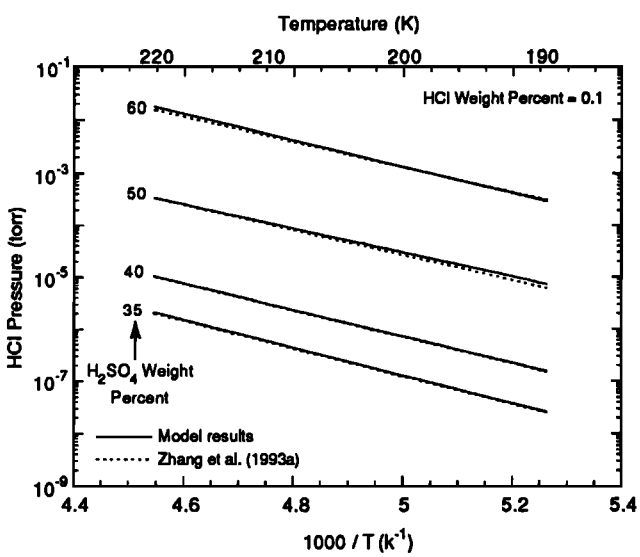

Figure 7. HCl vapor pressure over aqueous $H_2SO_4/HCl/H_2O$ solutions for a fixed HCl weight percent and various H_2SO_4 contents. Weight percents are indicated in the chart. Model results are shown as solid lines, and dashed lines are taken from *Zhang et al.* [1993a].

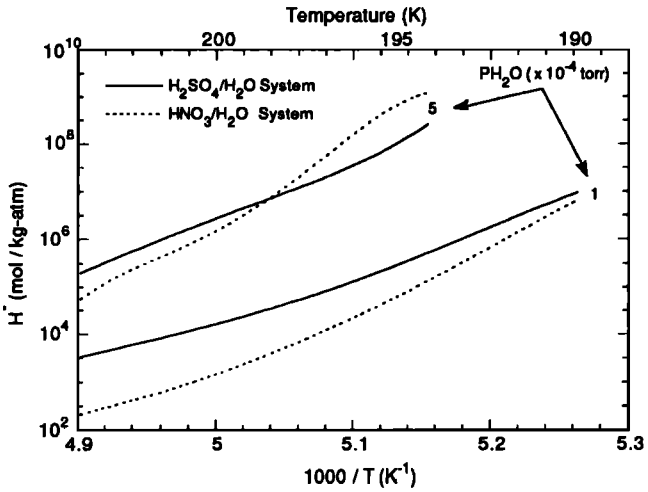

Figure 8. Effective Henry's law constant for HCl as a function of temperature in pure binary solutions of H_2SO_4/H_2O (solid lines) and HNO_3/H_2O (dashed lines) systems. Solid lines are calculated from (31), and dashed lines from (32); see text for detail. Model results are shown for two constant H_2O vapor pressure profiles as indicated in the chart. For model simulations, HNO_3 gas phase concentration was set at 2.0 x 10^{-7} torr.

H_2SO_4 weight percents > 60 and temperatures > 220 K, HBr is at least 100 times more soluble than is HCl (L. R. Williams, private communication, 1994). Therefore it is reasonable to assume that HBr is significantly more soluble in stratospheric aerosols than is HCl.

We have made a few assumptions about the mean pure binary activity of HBr in order to estimate its solubility in H_2SO_4 solutions. As stated above, current HBr binary activity data are not valid for stratospheric applications. However, by comparing the mean binary activity (equation (5)) of HCl with that of HBr in the limit where HBr coefficients are valid, we estimate that $\gamma^o_{HBr} \sim 10\gamma^o_{HCl}$ (for the higher molalities). Using this relation in (23) and (24), the H^* for HBr can be approximated from

$$H^*_{HBr} = \frac{m_{Br}}{P_{HBr}} = \frac{K_S(T)}{2m^o_S\left[\gamma^{mix}_{Br}(T, m^o_S)\right]^2} \tag{34}$$

where $\gamma^o_{HBr} \sim 10\gamma^o_{HCl}$, and γ^{mix}_{Cl} is given by (31b). Note at ~ 200 K, K_S for HBr is about 10,000 times larger than the K_S for HCl from (4). Thus, even though (34) is only a crude approximation, HBr is roughly 1000 times more soluble than is HCl in H_2SO_4 acid solutions for weight percents < 60 and T < 210 K (where it is reasonable to assume that H_2SO_4 is dissociated completely into SO_4^{2-}, see above). Model results for H^* of HBr are shown in Figure 6. Preliminary results suggest that HBr and HCl will at least have comparable aqueous phase concentrations in stratospheric aerosols despite the fact that HBr column abundance is about 1000 times less than that of HCl. Equilibrium measurements for the HBr ternary system, similar to that for the HCl [*Zhang et al.*, 1993a], are highly desirable, for improving our understanding on the solubility behavior of HBr in stratospheric aerosols.

4. Weak Univalent Acids in Aqueous Solutions

For weak acids in aqueous solutions, the strong electrolyte model is not applicable because there is a considerable amount of associated acid in solution. In the case of univalent weak acids, the dissolution in water leads to

$$HA(g) \overset{H}{\Leftrightarrow} HA(aq) \tag{35a}$$

$$HA(aq) \overset{K_a}{\Leftrightarrow} A^-(aq) + H^+(aq) \tag{35b}$$

where H is the physical Henry's law constant (mol/kg-atm), and K_a (mole/kilogram) is the dissociation constant. From (35), the effective Henry's law constant (H^*) is [*Seinfeld*, 1986]

$$H^*(T) = H(T)\left(1 + \frac{K_a(T)}{m(H^+)}\right) \tag{36}$$

Where $m(H^+)$ is the molality of the H^+ ion in solution. Note that the effect of dissociation is to "pull" more acid into solution than predicted on the basis of the physical Henry's law solubility alone. Therefore from K_a, H, and the pH of the solution, H^* can be estimated. Below, we discuss the applicability of (36) to the dissolution of HF and HOCl in H_2SO_4 solutions.

4.1. $H_2SO_4/HF/H_2O$ System

The solubility of HF in an aqueous solution can be estimated from (36), where the temperature dependent-functions are

$$\ln H(T) = 6.61712 + 3360.464/T - 0.02789T \tag{37a}$$

$$\ln K_a(T) = -12.6558 + 1599.7113/T \tag{37b}$$

These functions were derived from the enthalpy and the heat capacity change for reactions (35a) and (35b), and the standard temperature values for H and K_a [*Pitzer*, 1991; *Haung*, 1989; *Nordstrom et al.*, 1990].

For slightly acidic (pH > 4), neutral or basic pH, the dissociation of HF in solution can increase the solubility, which can be calculated from (36) and (37). However, for highly acidic solutions, the dissociation of HF has almost no impact on the HF solubility. Thus if (36) holds, then $H^* = H$. Due to lack of experimental data on the solubility of HF in concentrated H_2SO_4 solutions, we suggest using (37a) for calculating the solubility of HF in H_2SO_4 solutions. The variation of H with respect to temperature is depicted in Figure 6 based on equation (37a).

4.2. $H_2SO_4/HOCl/H_2O$ System

HOCl, like HF, is a weak acid, and its solubility in aqueous solutions can be estimated from (36). The physical Henry's constant for HOCl has been measured by *Blatchley et al.* [1992], and is equal to 16.667 atm^{-1} at 20°C. Here the Henry's constant (H_x) expresses the mole fraction (X) of HOCl over the equilibrium vapor pressure of HOCl, where $H = 1000H_x/18$ for $X << 1$. Using the heat of formation for HOCl in the gas [*Chase*, 1985] and the aqueous phase (*Lide*, 1990], the temperature dependence of the physical Henry's constant can be estimated from

$$\ln H = -10.989 + 5220.973/T \tag{38}$$

The effective Henry's law constant can now be calculated from (36). However, we could not find any data on the heat of formation for the OCl^- ion in the aqueous phase. Thus we were unable to estimate the temperature dependence for the dissociation constant. Therefore the effective Henry's law constant for HOCl can not be estimated at other temperatures.

Using the same arguments as above, we predict that in highly acidic solutions, the dissociation of HOCl has no impact on its solubility, and HOCl solubility can be estimated from (38). But recently, *Hanson and Ravishankara* [1993] determined the effective Henry's law constant for HOCl in H_2SO_4/H_2O solutions and showed that the solubility appears to depend on H_2SO_4 weight percent. However, the dependence of solubility on the H_2SO_4 weight percent, where $m(H^+)>1$ for all cases studied (Hanson and Ravishankara, 1993), can not be related to the acidity of the solution since $K_a / m(H^+) << 1$ (equation (36)). Therefore, from laboratory measurements, (35a) and (35b) are not adequate steps for describing the dissolution mechanism of HOCl in concentrated H_2SO_4 solutions.

From laboratory measurements [*Hanson and Ravishankara*, 1993], we suggest the following steps for dissolution of HOCl in concentrated H_2SO_4 acid solutions

$$HOCl(gas) \overset{H_{acid}}{\Leftrightarrow} HOCl(acid) \quad (39a)$$

$$HOCl(acid) + SO_4^{2-}(acid) \overset{K_{acid}}{\Leftrightarrow} HSO_4^-(acid) + OCl^-(acid) \quad (39b)$$

where we used the "acid" notation for solubility in H_2SO_4 solutions to distinguish it from the "aq" which refers to dissolution in the aqueous solution. H_{acid} is the physical Henry's constant for a H_2SO_4 solution at a given molality, m_s, and K_{acid} is the dissociation constant in the sulfuric acid solution. From the steps above, the effective Henry's law constant is

$$H^*_{acid} = H_{acid}(T, m_S)\left(1 + \frac{K_{acid}(T) m(SO_4^{2-})}{m(HSO_4^-)}\right) \quad (40)$$

where the solubility depends on the molality ratio of the bisulfate ion to the hydrogen sulfate ion. Note that as the H_2SO_4 solution becomes more concentrated, this ratio becomes smaller and H^*_{acid} approaches H_{acid}. Of course, to make predictions for HOCl solubility from (40), the physical Henry's constant and the dissociation constant must be determined in H_2SO_4 solutions from laboratory measurements. However, this formulation can explain the dependence of HOCl solubility, as observed by *Hanson and Ravishankara* [1993]. We have approximately fitted the H^*_{acid} data from Hanson and Ravishankara to a linear function in H_2SO_4 molality (m_s), given as

$$\ln H^*(T, m_S) = A_0(m_S) + \frac{A_1(m_S)}{T} \quad (41)$$

where A coefficients are given in Table 9. Figure 9 shows the calculated values of H^* for a number of H_2SO_4 solutions from (41). The dashed line shows the solubility predicted by HOCl dissolution in an aqueous solution from (38). Thus for less concentrated solutions (< 45 % H_2SO_4 by weight), H_2SO_4 might enhance the solubility of HOCl. For simple application to the stratosphere, the H^* for HOCl can be computed by substituting (21) into (41). Results of calculation for the H^* of HOCl in aqueous H_2SO_4 solutions are shown in Figure 6.

5. Stratospheric Implications and Volcanic Effects

As shown above, the composition of stratospheric aerosols is very sensitive to the relative humidity. However, equilibrium compositions also vary as a function of the total amount of HNO_3 and H_2SO_4 present per unit volume of air. To study the impact of all variables involved, we calculated variations in the aerosol composition as a function of temperature for five different cases (Table 10). The results are shown in Figure 10, where case I is for a typical condition at ~ 16 km altitude. The solid lines are calculated from (21), and the dashed lines are calculated from solving the ternary system of $H_2SO_4/HNO_3/H_2O$, as described above.

Molina et al. [1993] have shown that ternary bulk solutions with similar compositions as shown in Figure 10 can freeze under laboratory conditions. Whereas, for equivalent aqueous H_2SO_4 solutions (solid lines in Figure 10), the freezing temperature is observed to be near the ice frost point [*Zhang et al.*, 1993b; *Middlebrook et al.*, 1993]. The freezing of these ternary solutions may lead to the nucleation of NAT clouds in the stratosphere, as indicated by Molina et al.. In the laboratory, ternary bulk solutions (sample volumes ~ 5 μl - 5 ml) froze in about one hour when they were held at their equilibrium temperatures. In the atmosphere, the volume of a particle with a radius of about 1 μm is ~ 4 x 10^{-12} ml. According to the nucleation theory, the probability for homogeneous freezing of a solution depends strongly on the volume of the sample. The volume of the laboratory samples were about 10^8 to 10^{12} times larger than the volume of a particle with a radius of ~ 1 μm. Therefore, it is possible for ternary droplets to remain supercooled instead of nucleating into NAT particles under stratospheric conditions. However, more work is needed to demonstrate such freezing of aerosols as suggested by Molina et al.. Below we discuss solubilities and reactivities of various species in stratospheric aerosols, assuming that aerosols remained supercooled above the ice frost point.

Table 9. Effective Henry's Coefficients for HOCl

	$A_i(m_S) = a_o + a_1 m_S + a_2 m_S^2 + a_3 m_S^3$			
Coefficients	a_o	a_1	a_2	a_3
A_o	-3.8542280588*e*+1	8.0306114742*e*+0	-6.6982627997*e*-1	1.8577458295*e*-2
A_1	1.1723617497*e*+4	-2.3102480134*e*+3	1.9422695893*e*+2	-5.4624379476*e*+0

Read -3.8542280588*e*+1 as -3.8542280588 x 10^1.

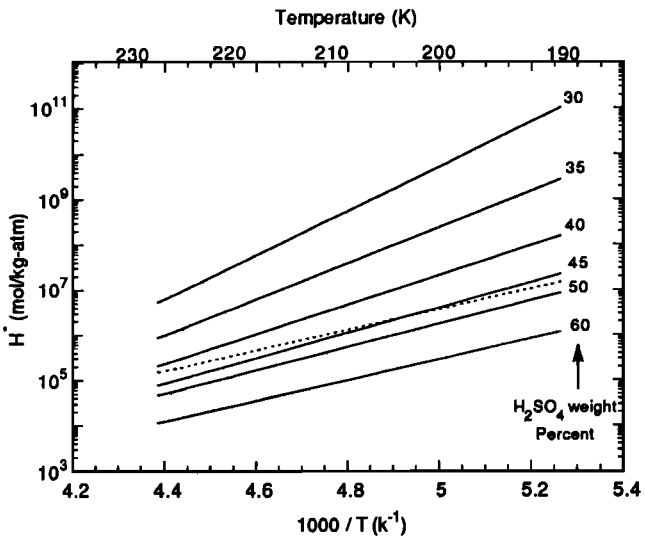

Figure 9. Effective Henry's law constant for HOCl as a function of temperature in aqueous H_2SO_4 solutions (solid lines). Solid lines are calculated from (41) based on *Hanson and Ravishankara*'s data [1993], as described in the text. The dashed line is the pure aqueous physical Henry's law constant calculated from (38).

5.1. Background Conditions

Figure 10a shows a typical composition of stratospheric aerosols at ~ 16 km altitude. From (18), the condensation point of the HNO_3/H_2O solutions for case I (Table 10) is about 195 K, which corresponds approximately to the maximum of the HNO_3 weight percent curve in Figure 10a. A comparison of Figure 10a with Figure 10b shows that lowering the HNO_3 concentration by one-half slightly changes the ternary aerosol composition, and the maximum for the weight percent of the HNO_3 curve is shifted by ~ 1 K. For case II, the condensation point of the HNO_3/H_2O solution is ~ 194 K from (18). For case III (Figure 10c), the water mixing ratio was decreased to one-half that for case I (Figure 10a). This results in a significant change in the aerosol composition, and the maximum of the HNO_3 weight percent curve is shifted by ~ 3 K compared to case I. The condensation point of the HNO_3/H_2O solution from (18) is ~ 192 K for case III. Therefore, it appears that, as the condensation point of the HNO_3/H_2O solution is approached, the background aerosols can rapidly uptake HNO_3. This HNO_3 uptake is also accompanied by H_2O vapor absorption, which results in the growth of background aerosols.

We also calculated the supersaturation (S) of HNO_3 over the NAT phase from *Hanson and Mauersberger* 's [1988b] empirical equation for cases I through III, where $S = 1$ at ~ 199.6, 198.7, and 196.3 K, respectively. At these temperatures, the ternary aerosols contain < 10 % HNO_3 by weight, and are ~ 4 K warmer with respect to the condensation point of HNO_3/H_2O solutions (Figure 10). As indicated above, as the condensation point of the HNO_3/H_2O solution is approached, aerosols can rapidly uptake HNO_3 and grow in size. If the aerosol is liquid when $S = 1$, then HNO_3 dissolution prevents the formation of a NAT embryo on the particle surface and therefore NAT can not grow from the gas phase onto the aerosol surface . From the NAT frost point (S ~ 1) to the intersection point (S ~ 10) in Figure 10 for cases I through III, the total HNO_3 uptake by the particles can contribute only slightly to the deliquescing of the background aerosols. But, from the intersection point to the ice frost point (~ 192.5 K for cases I and II; ~ 189 K for case III), the aerosols could grow to sizes that are significantly larger than those of the average background mode (about 0.1 μm radius) (A. Tabazadeh et al., submitted manuscript). Many Arctic field investigations showed that significant particle growth was not evident until S was about 10 [*Dye et al.*, 1992; *Kawa et al.*, 1992; *Pueschel et al.*, 1992]. These apparent supersaturations were observed primarily because significant particle growth is expected to occur only for S values > 10, if the aerosols remain as supercooled droplets (A. Tabazadeh et al., submitted manuscript).

5.2. Volcanic Conditions

Figures 10d and 10e demonstrate aerosol compositions under volcanic conditions, where the background sulfur concentration is increased by a factor of 10 and 100, respectively. For cases IV and V, the HNO_3/H_2O condensation point is ~ 195 K; therefore, an increase in the HNO_3 uptake is noted at ~ 195 K. Under volcanic conditions aerosols contain more H_2SO_4 than they do under background conditions (case I). However, under drastic volcanic conditions (Figure 10e), there is a significant difference between volcanic aerosol and background compositions. Also, the sulfur burden is so high that the HNO_3 concentration never exceeds that of H_2SO_4 for the conditions assumed for case V (Figure 10e).

Observational data of Mount Pinatubo aerosols suggest that volcanic aerosols remained supercooled instead of freezing to

Table 10. Model Conditions

Conditions		Case I	Case II	Case III	Case IV	Case V
HNO_3	mixing ratio, ppbv	10.0	5.0	10.0	10.0	10.0
H_2O	mixing ratio, ppmv	5.0	5.0	2.5	5.0	5.0
H_2SO_4	total mass, μg/m^3 of air	0.036	0.036	0.036	0.36	3.6
Total pressure, mbar		100.0	100.0	100.0	100.0	100.0

Abbreviations ppbv and ppmv are parts per billion by volume and parts per million by volume, respectively.

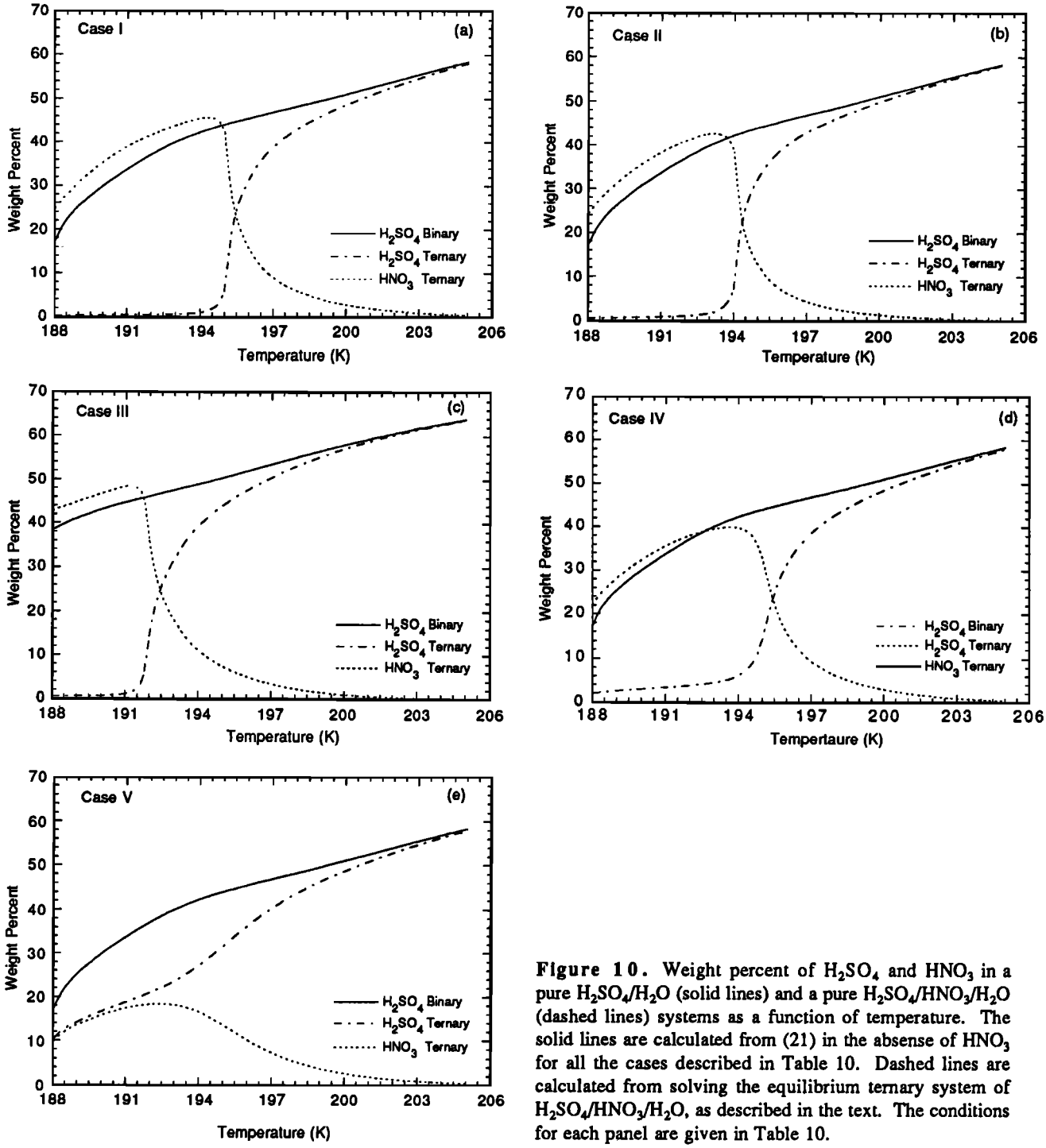

Figure 10. Weight percent of H_2SO_4 and HNO_3 in a pure H_2SO_4/H_2O (solid lines) and a pure $H_2SO_4/HNO_3/H_2O$ (dashed lines) systems as a function of temperature. The solid lines are calculated from (21) in the absense of HNO_3 for all the cases described in Table 10. Dashed lines are calculated from solving the equilibrium ternary system of $H_2SO_4/HNO_3/H_2O$, as described in the text. The conditions for each panel are given in Table 10.

form NAT particles [*Toon et al.*, 1993]. Pinatubo aerosols froze at ~ 190 K, which was near the ice frost point. In addition, recently *Deshler et al.* [1994] indicated that the physical characteristics of PSCs change significantly in the presence of volcanic aerosols. The PSC particles observed in Pinatubo clouds by Deshler et al. were usually < 1.0 μm in radius and more abundant than PSCs observed when volcanic aerosols were absent. These PSCs were probably ternary supercooled droplets instead of NAT particles, which are usually > 1.0 μm in radius. Hence, volcanic aerosols having similar compositions to the ones shown in Figure 10e may remain supercooled at temperatures above the ice frost point in the stratosphere.

5.3. Aerosol Scavenging

Assuming that H_2SO_4 is present only in the aerosol phase, the scavenging efficiency (r) of species X can be scaled with respect to the total mass of H_2SO_4 present per unit volume of air, given as

$$r = \frac{L_{WC} m_X N_A}{X_g^o} \tag{42a}$$

$$L_{WC} = \text{mass}_s x 10^{-12} / 98 m_s \tag{42b}$$

where L_{WC} is the total liquid water content (kg) present per cubic centimeter of air, X_g^o is the gas phase concentration of

species X (# / cm^3), N_A is the Avagadro's number, m_X is the molality of species X in solution, mass$_s$ is total mass of H_2SO_4 (μg / m^3 of air), and m_s is the molality of H_2SO_4 in the aerosol phase. Below, we used (42a) and (42b) to calculate the efficiency of stratospheric aerosols in the removal of gas phase species.

Using HNO_3 ternary compositions shown in Figure 10 in (42), we calculated the HNO_3 scavenging efficiency by stratospheric aerosols. The results are shown in Figure 11. For cases I, II, III, and IV (Table 10), the HNO_3 gas phase concentration decreases after the intersection point is reached in Figure 10. From the intersection point to the ice frost point (~ 192.5 K for cases I, II, and IV; ~ 189 K for case III), about 50 % to 80% of the HNO_3 gas column can be scavenged by the aerosol phase (Figure 11). For case V, where the total mass of HNO_3 and H_2SO_4 present per unit volume of air are roughly equal (~ 3.5 μg / m^3 of air), the HNO_3 column can be depleted by aerosols even at higher temperatures. From Figure 11, at about 196 K, the HNO_3 column is depleted by ~ 50% , observed by *Toon et al.* [1993]. In addition, *Coffey and Mankin* [1993] observed that, in the volcanic clouds of El Chichon and Pinatubo, the heterogeneous conversion of N_2O_5 into HNO_3 by volcanic aerosols did not correspond to an equal increase in the HNO_3 column abundance. This may be explained by the volcanic aerosol scavenging of HNO_3 for $T <$ 200K.

The solubility of HCl in stratospheric aerosols is illustrated in Figure 12 for the cases mentioned above (Table 10). The solubilities were calculated directly from (33), using the H_2SO_4 and HNO_3 concentrations shown in Figure 10. HCl scavenging was calculated from (42a) and (42b) assuming X_g^o ~ 5 x 10^9 / cm^3. For cases I and II at 193 K, the H^* for HCl is ~ 10^9 mol / kg-atm, which is a factor of 5 larger than if a pure H_2SO_4/H_2O composition is assumed for the aerosols (Figure 12). We used H^* values for HCl shown in Figure 12 at 193 K to calculate the HCl solubility in solution. The calculated HCl molality in solutions is ~ 0.13 m. Using this molality in (42a) for cases I and II, ~ 6 % of the HCl gas column can be scavenged by the aerosols at about 193 K. At 192.5 K (~ ice frost point), ~ 12 % of the HCl can be depleted from the gas phase by the aerosols. For case III, similar depletions of the

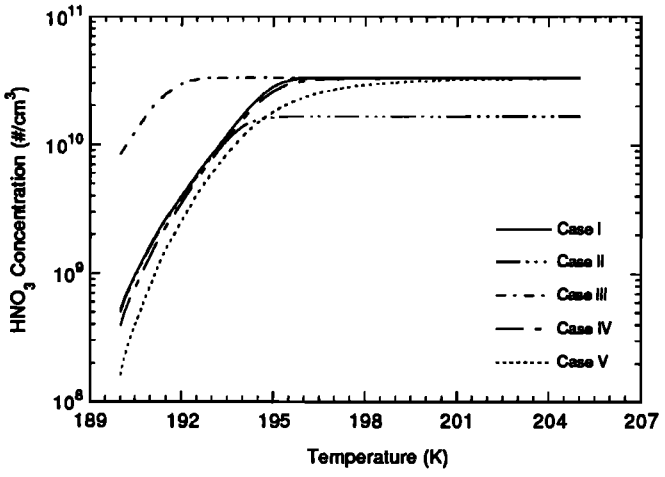

Figure 11. Equilibrium HNO_3 gas phase concentration variation as a function of temperature over supercooled ternary solutions of $H_2SO_4/HNO_3/H_2O$. The conditions for each case are given in Table 10.

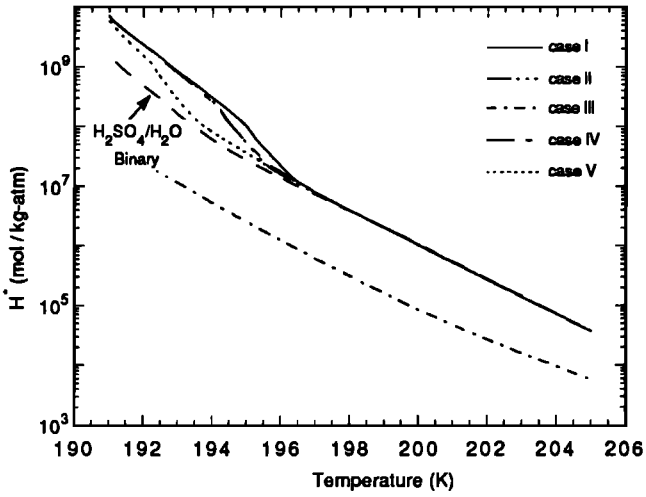

Figure 12. Effective Henry's law constant for HCl as a function of temperature. The conditions for each case are given in Table 10. The line corresponding to the effective Henry's law constant in the absence of HNO_3 for case I is calculated from (31) and is labeled in the chart as H_2SO_4/H_2O binary.

HCl column (~ 6 % to 12 %) are calculated at about 189 K (~ ice frost point) to 190 K.

For case VI at 193 K, the HCl solubility in solution (0.13 *m*) and the liquid water content are similar to that of case I. Thus, HCl column can be depleted by ~ 6 % at 193 K and ~ 12 % at 192.5 K. For case V, the HCl solubility (H^* ~ 3 x 10^8 mol / kg-atm) is lower in the volcanic aerosols than in aerosols described in case I. The calculated HCl molality in solution for case V at 193 K is roughly 0.04 *m*. However, the liquid water content of the aerosols per unit volume of air is about 2.5 times larger for case V than for case I. Using this HCl molality in (42a), the HCl column can be depleted by about 5 % at ~ 193 K. However, as the temperature approaches the ice frost point (~ 192.5K), the H^* can increase by a factor of 3, which can cause a 15 % depletion of the HCl gas column. If ice does not crystallize at ~ 192.5 K in the volcanic aerosols, then the HCl column can be depleted by about 30 % at ~ 192 K from (42a). *Toon et al.* [1993] observed a 30 % depletion of the HCl column in the dense volcanic clouds of Pinatubo, which may be related to the volcanic aerosol scavenging of HCl. Further, they also suggested that the depletion of the HCl gas column could have been caused by the chemical processing of HCl in the volcanic aerosols, as described below. In fact, both factors (scavenging and chemical processing of HCl) may have contributed some to the depletion of the HCl column as observed by *Toon et al.* [1993].

The scavenging efficiency of HBr by stratospheric aerosols can be approximated from (34) and (42a). We emphasize that the accuracy of (34) must be validated against laboratory observations. Assuming X_g^o ~ 5 x 10^6 / cm^3 for the HBr gas phase concentration, the HBr gas column can be depleted by about 100 % at ~192.5 K (ice frost point) for cases I, II, IV and V. For case III similar depletions are calculated at ~ 189 K. The total mas of HBr in the stratosphere is about 5 x 10^{-4} μg / m^3 of air, which is roughly 70 times smaller than the background H_2SO_4 mass (Table 10). Thus, even if all the HBr column is incorporated into the aerosols, the HBr aqueous

concentration is always roughly 70 times smaller than the H_2SO_4 aqueous concentration. For example, for case I at 193 K, the H_2SO_4 weight percent in solution is ~ 0.5% (Figure 10a). Therefore, if we assume that all the available HBr is in the aqueous phase, it can contribute only 0.0070 % to the total aerosol mass. However, the HBr aqueous concentration can be about 10^{-3} *m*, which may result in a rapid chemical processing of HBr, as described below.

In the case of many in situ measurements, the X/HF ratio is used as an indicator of the chemical removal of X [*Toon et al.*, 1993]. This holds if HF is chemically inert. However, if considerable amount of HF is scavenged by the aerosol phase, the X/HF ratio should be modified. When calculating the scavenging efficiency of HF, it is important to note that (37a) might not be valid for acidic solutions. Due to a lack of laboratory data, we used (37a), and (42a) to estimate the scavenging efficiency of HF by stratospheric aerosols. From (37a), the aqueous phase Henry's constant for HF is ~ 10^8 mol / kg-atm (for T < 193 K), which we have used in (42a) to calculate the scavenging efficiency of HF. Assuming X_g^o ~ 5 x 10^9 / cm^3 for the HF gas phase concentration, the calculated HF molality in solution is about 0.01 *m* for T < 193 K. For cases I through V (Table 10), the HF gas column can be depleted by ~ 1 % before the ice frost point is reached. However, if HF dissolution in H_2SO_4 solutions is similar to that of HOCl, then its effective Henry's constant could be a factor of 10 larger in dilute H_2SO_4 solutions (see Figure 9) compared to the pure aqueous phase physical Henry's constant used here. Therefore, up to a 10 % scavenging of HF by the aerosols at low temperatures may not be ruled out in case V. Under a volcanic condition, where H_2SO_4 aqueous concentration is significant at low temperatures, HF can reversibly react with sulfate ions in solution, increasing the solubility of HF. Laboratory observations on the solubility behavior of HF in aqueous HNO_3 and H_2SO_4 solutions are needed to narrow the uncertainty associated with using the X/HF ratio.

5.4. Chemistry In/on Supercooled Droplets

The HCl aqueous concentration in supercooled aerosols may be as high as 0.1 *m*, which may result in a rapid chemical processing of HCl in solution. Recently, *Hanson and Ravishankara* [1993] determined that the aqueous phase reaction rate constant for HCl + HOCl reaction is k ~ 10^5 L / mol-s (~ 10^5 kg of water / mol-s). Thus the reaction rate in the bulk can be computed as

$$R = k[\mathrm{HCl}][\mathrm{HOCl}] \qquad (43)$$

where the bracketed quantities are aqueous phase concentrations.

For cases I and II, the liquid water content is ~ 4 x 10^{-15} kg / cm^3 of air from (42b) and the HCl aqueous concentration is about 0.1 *m* at 193 K (assuming X_g^o ~ 5 x 10^9 / cm^3). The HOCl solubility in solution at 193 K for cases I and II (almost pure HNO_3/H_2O solutions, see Figures 10a and 10b) may be lower than that estimated from (41) because HOCl in solution probably does not reversibly react with nitrate ions as it does with sulfate ions (see above). Therefore, we used (38) instead of (41) to calculate the HOCl Henry's law constant for cases I and II, which is ~ 10^7 mol / kg-atm (see the dashed line in Figure 9). For an HOCl gas phase concentration of about 10^5 / cm^3, the HOCl aqueous concentration is ~ 10^{-8} *m*. Hence from (43) and (42b), 2.4 x 10^5 Cl_2 molecules may be produced every second per cubic centimeter of air. Also, for volcanic conditions (case V), where the aerosols contain more H_2SO_4 in solution, the effective Henry's constant for HOCl may be a factor of 10 larger (~ 10^8 mol / kg-atm, see Figure 9). This can result in a rapid chemical processing of HCl in solution, which may have contributed some to the depletion of the HCl column, in the volcanic clouds of Pinatubo, as observed by *Toon et al.* [1993].

Hanson and Ravishankara [1991] have parameterized the reaction probability (number of molecules that react on the surface (or bulk) / gas kinetic flux) for the $ClONO_2 + H_2O$ reaction as a function of H_2SO_4 weight percent in solution ($\log \gamma_m = 1.86 - 0.0747 W_s$, where γ_m is the reaction probability and W_s is the weight percent of H_2SO_4 in solution). Assuming an aqueous H_2SO_4 composition for the droplets for case I (solid curve in Figure 10a), the H_2SO_4 weight percent varies from ~ 60 % at 206 K to ~ 36 % at 192.5 K (ice frost point). The reaction probability for the hydrolysis of $ClONO_2$ increases by a factor 60 as the temperature decreases from 206 to 192.5 K. For conditions of case I, the relative humidity (RH = 100 x ambient water vapor pressure (torr) / equation (11)) varies from 7 to 43 % as the temperature decreases from 206 to 192.5 K. Therefore, increasing the RH over the aerosol surface by a factor of 6 can lead to an increase in the reaction efficiency by a factor of 60. *Abbatt and Molina* [1992] have observed that the efficiency of $ClONO_2$ reactions on NAT surfaces also increased as the RH over the surface increased. Recently, we calculated that an increase in the RH over a NAT surface from 6.7 % to 50 % increased the efficiency of $ClONO_2$ reactions on NAT surfaces by a factor of about one-hundred [*Tabazadeh and Turco*, 1993]. We attribute this to an increase in the abundance of adsorbed water layers on NAT surfaces.

From the similarities between reactions of $ClONO_2$ on NAT and on aqueous H_2SO_4 surfaces described here, we conclude that $ClONO_2$ hydrolysis probably occurs on the surface of H_2SO_4 solutions. Also, the reaction probability is controlled by the activity of water over the aerosol surface rather than the aerosol composition. Therefore, the reaction probability for this heterogeneous process calculated on pure aqueous H_2SO_4 solutions [*Hanson and Ravishankara*, 1991] is probably valid for all the ternary compositions shown if Figure 10 (ternary lines), as long as a weight percent of a pure aqueous H_2SO_4 solution (solid line in Figure 10) is assumed for the calculations.

Abbatt and Molina [1992] have shown that the reaction probability for the $ClONO_2$ + HCl reaction is about 100 times larger than the $ClONO_2 + H_2O$ reaction on NAT surfaces. Under their laboratory conditions, HCl formed roughly a monolayer on NAT surfaces [*Tabazadeh and Turco*, 1993]. If $ClONO_2$ reactions occur on the surface of H_2SO_4 acid solutions, then the efficiency for the $ClONO_2$ + HCl reaction may be a factor of 100 larger than the $ClONO_2 + H_2O$ reaction. However, for a 0.1 *m* HCl solution (0.1 moles of HCl per 55.5 moles of H_2O), the HCl surface concentration is ~ 500 times smaller than is the H_2O surface concentration. This is significantly different from the conditions on a NAT surface, where HCl forms roughly a monolayer on the surface. Assuming 500 collisions of $ClONO_2$ molecules to an aerosol surface, only 1 collision will be with an HCl molecule (for a 0.1 *m* HCl solution). However, because the reaction with HCl is 100 times more efficient, about 20 % of the total number of effective

collisions with the surface may be the result of the direct HCl reaction with $ClONO_2$ (for 0.1 *m* HCl solution). If HCl concentration is 0.01 *m*, then only 2 % of the effective collisions are due to the $ClONO_2$ + HCl reaction. For HCl concentration < 0.01 *m*, the direct reaction of the $ClONO_2$ + HCl on the surface may be negligible compare to the $ClONO_2$ + H_2O reaction.

The reaction probability for the hydrolysis of $ClONO_2$ on stratospheric aerosols is about 0.1 [*Hanson and Ravishankara*, 1991] at low temperatures, which rapidly produces HOCl on the aerosol surface. This heterogeneous process may significantly increase the HOCl pressure over the surface of a droplet and therefore increase the HOCl concentration in solution, enhancing the rate of the HCl + HOCl bulk phase reaction, described above. In addition, we calculated an aqueous concentration for HBr of about 10^{-3} *m* in the aerosols for T < 193 K (see above). Therefore, if we assume a bulk phase reaction rate constant of ~ 10^5 L / mol-s for the HBr + HOCl reaction (same as that of the HCl + HOCl reaction), then this process may also contribute to the production of reactive halogen species.

6. Conclusions

In this paper we presented the first thorough study on the composition of stratospheric aerosols. Our results show that, for temperatures below 200 K, HNO_3 is a major component of stratospheric aerosols. Here we discussed some of the effects caused by HNO_3 dissolution on the physical and chemical properties of stratospheric aerosols. For instance, after large volcanic eruptions, such as Pinatubo, the composition of stratospheric aerosols could be different from background compositions. We predicted that these solutions do not freeze until at least the ice frost point is reached, and they may significantly scavenge HNO_3 and HCl from the gas phase. Further, in volcanically disturbed periods, different types of PSC particles (ternary solutions of $H_2SO_4/HNO_3/H_2O$) may exist. The chemistry occurring in these droplets may be quite different from the heterogeneous chemistry occurring on NAT surfaces. Currently, we are developing a model to describe the mechanism at which chlorine- and nitrogen-containing compounds react on both the surfaces and in the bulk of stratospheric aerosols. Previously, we constructed a surface-chemistry model to investigate the mechanism at which NAT and ice particles activated chlorine compounds [*Tabazadeh and Turco*, 1993]. These models are essential to aid our understanding, on the microscopic level, about the nature of physical-chemical processes responsible for the changes in the stratospheric composition and ozone abundance.

Acknowledgments. We wish to thank O. Toon, R. Zhang, M. Molina, A. Middlebrook, M. Tolbert, L. Williams, D. Golden, B. Luo, S. Clegg, T. Peter, R. Müller, P. Crutzen, D. Hanson, and A. Ravishankara for preprints of their work. This research was supported by NASA's Upper Atmosphere Program under grant NAGW-2183 and the NSF Atmospheric Chemistry program under grant ATM-9216646 . One of us [AT] is supported by a NASA Graduate Fellowship in Global Change Research under grant NGT-30079.

References

Abbatt, J. P., Molina, M. J., Heterogeneous interactions of $ClONO_2$ and HCl on nitric acid trihydrate at 202 K", *J. Phys. Chem.*, *96*, 7674-7679, 1992.

Bassett, M., and J. H, Seinfeld, Atmospheric equilibrium model of sulfate and nitrate aerosols, *Atmos. Environ.*, *17*, 2237-2252, 1983.

Blatchley, E. R., III, R. W. Johnson, J. E. Alleman, and W. F. McCoy, Effective Henry's law constants for free chlorine and free bromine, *Water Res.*, *26*, 99-206, 1992.

Brimblecombe, P., and S. L. Clegg., The solubility and behavior of acid gases in the marine aerosols, *J. Atmos. Chem.*, *7*, 1-18, 1988.

Bromley, L. A., Thermodynamic properties of strong electrolytes in aqueous solutions, *AIChE J.*, *19*, 313-320, 1973.

Chase, M. W., JANAF thermochemical tables (supplement no. 1), *J. Phys. Chem. Ref. Data*, *14*, 744, 1985.

Clegg, S. L., and P. Brimblecombe, Equilibrium partial pressure and mean activity and osmotic coefficients of 0-100 % nitric acid as a function of temperature, *J. Phys. Chem.*, *94*, 5369-5380, 1990.

Clegg, S. L., and P. Brimblecombe, Correction to equilibrium partial pressure and mean activity and osmotic coefficients of 0-100 % nitric acid as a function of temperature paper, *J. Phys. Chem.*, *96*, 6854, 1992.

Coffey, M. T., and W. G. Mankin, Observation of the loss of stratospheric NO_2 following volcanic eruptions, *Geophys. Res. Lett.*, 20, 2873-2876, 1993.

Deshler, T., B. J. Johnson, and W. R. Rozier, Changes in the character of polar stratospheric clouds over Antarctica in 1992 due to the Pinatubo volcanic aerosols, *Geophys. Res. Lett.*, *21*, 273-276, 1994.

Dye, J. E., D. Baumgardner, B. W. Gandrud, S. R. Kawa, K. K. Kelly, M. Loewenstein, G. V. Ferry, K. R. Chan , and B. L. Gary, Particle size distribution in Arctic polar stratospheric clouds, growth and freezing of sulfuric acid droplets, and implications for cloud formation, *J. Geophys. Res.*, *97*, 8015-8034, 1992.

Fritz, J. J., and C. R. Fuget, Vapor pressure of aqueous hydrogen chloride solutions, 0°C to 50°C, *Ind. Eng. Chem. Res.*, *1*, 10-12, 1956.

Gmitro, J. L., and T. Vermeulen, Vapor-liquid equilibria for aqueous sulfuric acid, *AIChE J.*, *10*, 740-746, 1964.

Granier, C., and G. Brasseur, Impact of heterogeneous chemistry on model predictions of ozone change, *J. Geophys. Res.*, *97*, 18,015-18,033, 1992.

Hammer, W. J., and Y.C. Wu, Osmotic coefficients and mean activity coefficients of univalent electrolytes in water at 25 °C, *J. Phys. Chem. Ref. Data*, *1*, 1047-1099, 1972.

Hanson, D., The vapor pressure of super cooled HNO_3/H_2O solutions, *Geophys. Res. Lett.*, *17*, 421-423, 1990.

Hanson, D., and K. Mauersberger, Vapor pressures of HNO_3/H_2O solutions at low temperatures, *J. Phys. Chem.*, *92*, 6167-6170, 1988a.

Hanson, D., and K. Mauersberger, Laboratory studies of nitric acid trihydrate: Implications of south polar stratosphere, *Geophys. Res. Lett.*, *15*, 855-858, 1988b.

Hanson, D. R., and A. R. Ravishankara, The reaction probability of $ClONO_2$ and N_2O_5 on 40 to 75 % sulfuric acid solutions, *J. Geophys. Res.*, *96*, 17,307-17,314, 1991.

Hanson, D. R., and A. R. Ravishankara, The uptake of HCl and HOCl onto sulfuric acid: Solubilities, diffusivities, and reaction, *J. Phys. Chem.*, *97*, 12,309-12,315, 1993.

Haung, H., Estimations of Pitzer's ion interaction parameters for electrolytes involved in complex formation using a chemical equilibrium model, *J. Solution Chem.*, *18*, 1069, 1989.

Hofmann, D. J., and S. Solomon, Ozone destruction through heterogeneous chemistry following the eruption of El Chichon, *J. Geophys. Res.*, *94*, 5029-5040, 1989.

Holmes, H. F., R. H. Busey, J. M. Simonson, R. E. Mesmer, D. G. Archer, and R. H. Wood, The enthlapy of dilution of HCl (aq) to 648 K and 40 MPa / Thermodynamic properties, *J. Chem. Thermodyn.*, *19*, 863-890, 1987.

Jaecker-Voirol, A., J. L. Ponche, and P. Mirabel, Vapor pressures in the ternary system water-nitric acid-sulfuric acid at low temperatures, *J. Geophys. Res.*, *95*, 11,857-11,863, 1990.

Kawa, S. R., D. W. Fahey, K. K. Kelly, J. E. Dye, D. Baumgardner, B. W. Gandrud, M. Loewenstein, G. V. Ferry, and K. R. Chan, The Arctic polar stratospheric cloud aerosol: Aircraft measurements of reactive nitrogen, total water, and particles, *J. Geophys. Res.*, *97*, 7925-7938, 1992.

Kusik, C. L., and H. P. Meissner, Electrolyte activity coefficients in inorganic processing, *AIChE Symp.Ser., 74*, 14-20, 1978.

Lide, D. R. (Ed.), *Handbook of Chemistry and Physics*, 71st ed., pp. 5-101-5-102, CRC Press, Boca Raton, Fla., 1990.

Luo, B. P., S. L. Clegg, T. Peter, R. Müller, and P. J. Crutzen, HCl solubility and liquid diffusion in aqueous sulfuric acid under stratospheric conditions, *Geophys. Res. Lett., 21*, 49-52, 1994.

Middlebrook, A. M., L. T. Iraci, L. S. McNeill, B. G. Koehler, M. A. Wilson, O. W. Saastad, and M. A. Tolbert., Fourier Transform-Infrared studies of thin H_2SO_4/H_2O films: Formation, water uptake, and solid-liquid phase changes, *J. Geophys. Res., 98*, 20,473-20,481, 1993.

Molina, M. J., R. Zhang, P. L. Wooldridge, J. R. McMahon, J. E. Kim, H. Y. Chang, and K. D. Beyer, Physical chemistry of the $H_2SO_4/HNO_3/H_2O$ system: Implications for polar stratospheric clouds, *Science, 261*, 1418-1423, 1993.

Nordstrom, D. K., N. L. Plummer, and D. Langmuir, Revised chemical equilibrium data for major water mineral reactions and their limitations, *Chemical Modeling in Aqueous Systems II*, edited by D. C. Melchior and R. L. Bassett, p. 398, American Chemical Society, Washington, D. C., 1990.

Pilinis, C., and J. H. Seinfeld, Continued development of a general model for inorganic multicomponent atmospheric aerosols, *Atmos. Environ., 21*, 2453-2466, 1987.

Pitzer, K. S., *Activity Coefficients in Electrolyte Solutions*, 2nd ed., pp. 12-13, CRC Press, Boca Raton, Fla., 1991.

Pitzer, K. S., R. N. Roy, and L. F. Silvester, Thermodynamics of electrolytes. 7. Sulfuric acid, *J. Am. Chem. Soc., 99*, 4930-4936, 1977.

Prather, M., Catastrophic loss of stratospheric ozone in dense volcanic cloud, *J. Geophys. Res., 97*, 10,187-10,191, 1992.

Pueschel, R. F., G. V. Ferry, K. G. Snetsinger, J. Goodman, J. E. Dye, D. Baumgardner, and B. W. Gandrud, A case of Type I polar stratospheric cloud formation by heterogeneous nucleation, *J. Geophy, Res., 97*, 8105-8144, 1992.

Reardon, E. J., and R. D. Beckie, Modeling chemical equilibria of acid mine-drainage: The $FeSO_4$-H_2SO_4-H_2O system, *Geochim. Cosmochim. Acta, 51*, 2355-2368, 1987.

Reihs, C. M., D. M. Golden, and M. A. Tolbert, Nitric acid uptake by sulfuric acid solutions under stratospheric conditions: Determination of Henry's law solubility, *J. Geophys. Res., 95*, 16,545-16,550, 1990.

Seinfeld, J., *Atmospheric Chemistry and Physics of Air Pollution*, chap 5, p. 202, Wiley, New York, 1986.

Solomon, S., R. R. Garcia, F. S. Rowland, and D. J. Wuebbles, On the depletion of Antarctic ozone, *Nature, 321*, 755-758, 1986.

Steele, H. M., and P. Hamill, Effects of temperature and humidity on the growth and optical properties of sulfuric acid-water droplets in the stratosphere, *J. Aerosol Sci., 12*, 517-528, 1981.

Stelson, A. W., and J. H. Seinfeld, Relative humidity and pH dependence of the vapor pressure of ammonium nitrate-nitric acid solutions at 25 °C, *Atmos. Environ., 16*, 993-1000, 1982.

Stokes, R. H., and R. A. Robinson, Interactions in aqueous nonelectrolyte solutions: I. Solute-solvent equilibria, *J. Phys. Chem., 70*, 2126-2130, 1965.

Tabazadeh, A., and R. P. Turco, A model for heterogeneous chemical processes on the surfaces of ice and nitric acid trihydrate particles, *J. Geophys. Res., 98*, 12,727-12,740, 1993.

Tolbert, M. A., M. J. Rossi, and D. N. Golden, Heterogeneous interaction of chlorine nitrate, hydrogen chloride, and nitric acid with sulfuric acid surfaces at stratospheric temperatures, *Geophys. Res. Lett., 15*, 847-850, 1988.

Toon O. et al., Heterogeneous reaction probabilities, solubilities, and the physical state of cold volcanic aerosols, *Science, 261*, 1136-1140, 1993.

Turco, R. P., and Hamill, P., Supercooled sulfuric acid droplets: Perturbed stratospheric chemistry in early winter, *Ber. Bunsen. Ges. Phys. Chem., 96*, 323-334, 1992.

Turco, R. P., O. B. Toon, and P. Hamill, Heterogeneous physicochemistry of the polar ozone hole, *J. Geophys. Res., 94*, 16,493-16,510, 1989.

Van Doren, J. M., L. R. Watson, P. Davidovits, D. R. Worsnop, M. S. Zahniser, and C. E. Kolb, Uptake of N_2O_5 and HNO_3 by aqueous sulfuric acid droplets, *J. Phys. Chem., 95*, 1684-1689, 1991.

Watson, L. R., J. M. Van Doren, P. Davidovits, D. R. Worsnop, M. S. Zahniser, and C. E. Kolb, Uptake of HCl molecules by aqueous sulfuric acid droplets as a function of acid concentration, *J. Geophys. Res., 95*, 5631-5638, 1990.

Williams, L. R., and D. M. Golden, Solubility of HCl in sulfuric acid at stratospheric temperatures, *J. Geophys. Res. Lett., 20*, 2227-2230, 1993.

Zeleznik, F., Thermodynamic properties of the aqueous sulfuric acid system to 350 K, *J. Phys. Chem. Ref. Data, 20*, 1157-1200, 1991.

Zhang, R., P. J. Wooldridge. J. P. D. Abbatt, and M. J. Molina, Vapor pressure measurements for the $H_2SO_4/HNO_3/H_2O$ and $H_2SO_4/HCl/H_2O$ systems: Incorporation of stratospheric acids into background sulfate aerosols, *J. Phys. Chem., 97*, 8541-8548, 1993a.

Zhang, R., P. J. Wooldridge, J. P. D. Abbatt, and M. J. Molina, Physical chemistry of the H_2SO_4/H_2O binary system at low temperatures: Stratospheric implications, *J. Phys. Chem., 97*, 7351-7358, 1993b.

M. Z. Jacobson, A. Tabazadeh, and R. P. Turco, Department of Atmospheric Sciences, University of California, Los Angels, 405 Hilgard Avenue, Los Angeles, CA 90024-1565.

(Received November 23, 1993; revised March 14, 1994;
accepted March 22, 1994)